Supplementary Information

Supramolecular X- and H-Shape Star Block Copolymers via Cyclodextrin-Driven Supramolecular Self-Assembly

*Bernhard V. K. J. Schmidt and Christopher Barner-Kowollik**

Preparative Macromolecular Chemistry, Institut für Technische Chemie und Polymerchemie, Karlsruhe Institute of Technology (KIT), Engesserstr. 18, 76128 Karlsruhe, Germany and Institut für Biologische Grenzflächen, Karlsruhe Institute of Technology (KIT), Hermann-von-Helmholtz Platz 1, 76344 Eggenstein-Leopoldshafen, Germany.

[*](C.B.-K.) Tel (+49) 721 608-45642; Fax (+49) 721 608-45740; e-mail: christopher.barner-kowollik@kit.edu

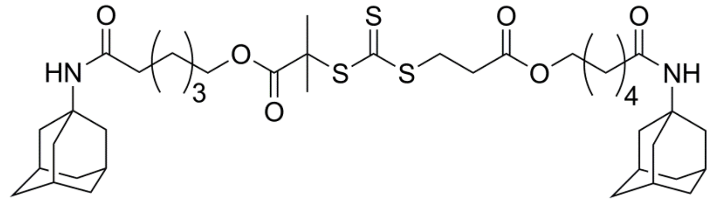

CTA1

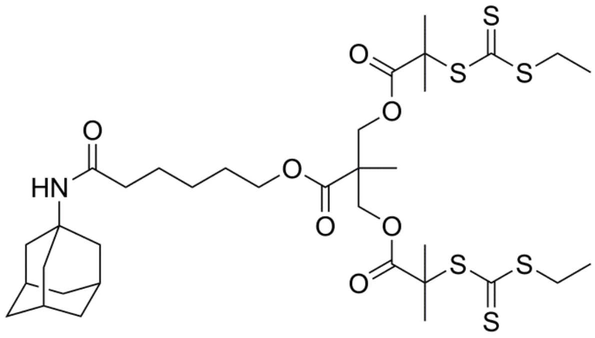

CTA2

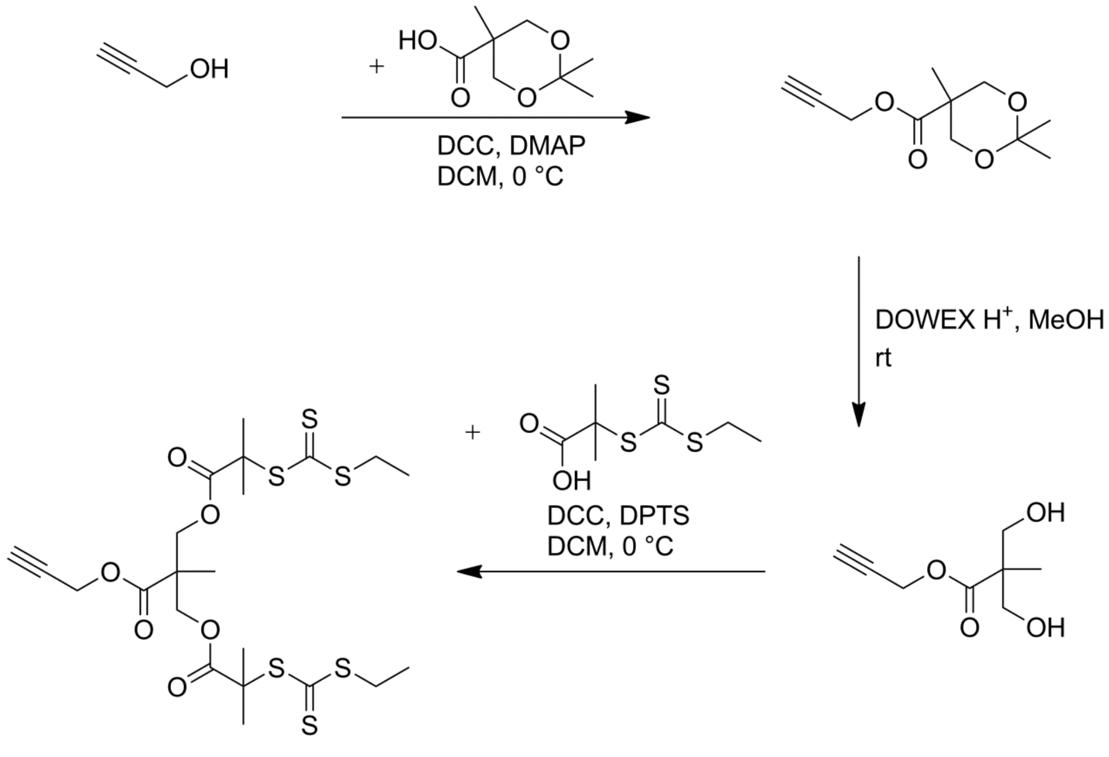

CTA3

Scheme S1. Structures of **CTA1** and **CTA2** and synthesis of **CTA3**.

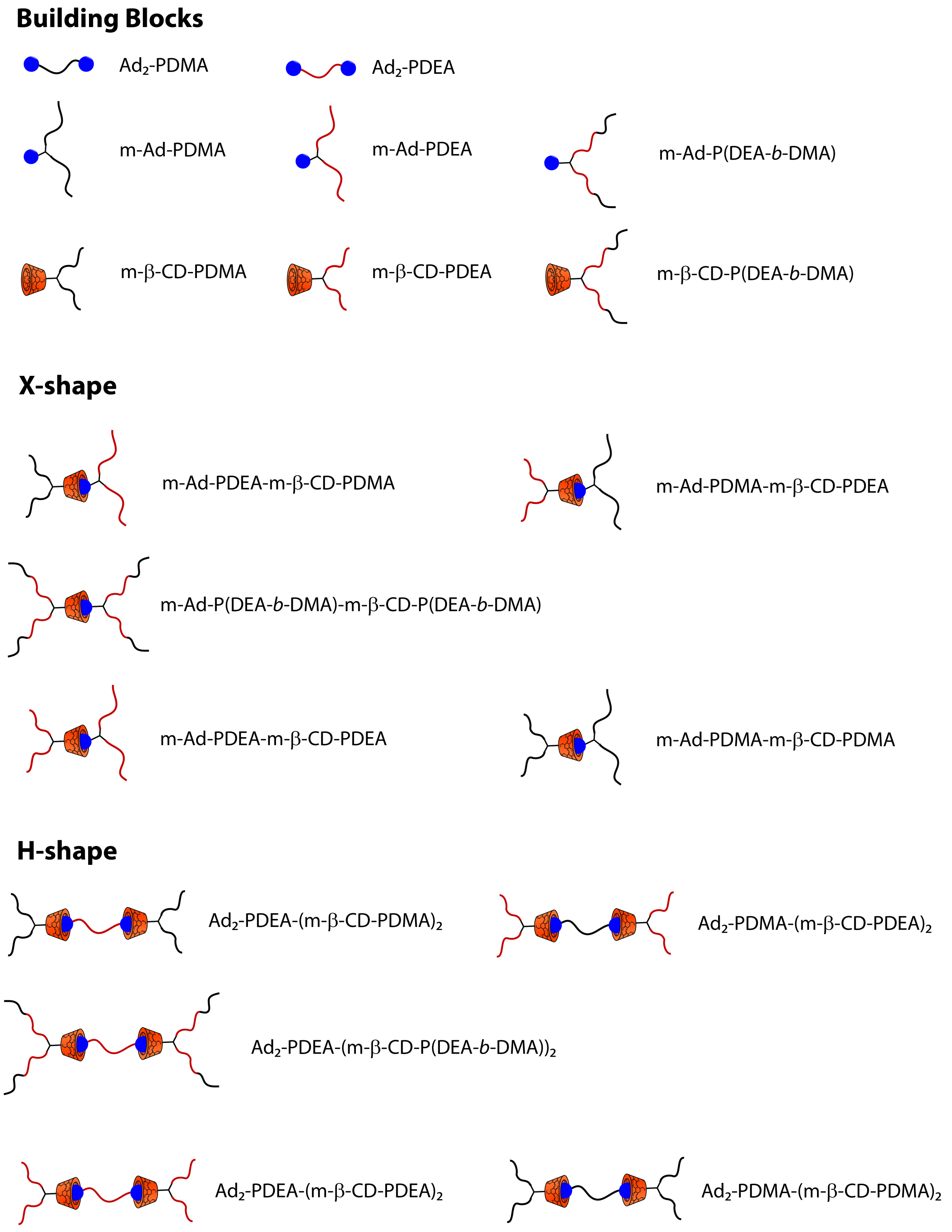

Scheme S2. Schematic overview of the utilized polymers and investigated supramolecular star polymers (PDMA: red, PDEA: black, adamantyl: blue sphere, CD: orange truncated cone).

Synthesis of Double Adamantyl Endfunctionalized PDMA (Ad$_2$-PDMA$_{57}$)

CTA1 (112.0 mg, 0.15 mmol, 1.0 eq.), DMA (500.0 mg, 5.05 mmol, 33.7 eq.), AIBN (4.7 mg, 0.03 mmol, 0.2 eq.), DMF (3.4 mL) and a stirring-bar were added into a Schlenk-tube. After three freeze-pump-thaw cycles the tube was backfilled with argon, sealed, placed in an oil bath at 60 °C and removed after 24 h. The tube was subsequently cooled with liquid nitrogen to stop the reaction. A NMR-sample was withdrawn for the determination of conversion and $CDCl_3$ was added. A quantitative conversion was calculated based on the NMR data (see Characterization Methods for details of the calculation). The residue was dialysed against deionized water with a SpectraPor3 membrane (MWCO = 1000 Da) for 3 days at ambient temperature. The solvent was removed in vacuo to yield Ad$_2$-PDMA$_{57}$ as a yellow solid (0.41 g, 67%, $M_{\mathrm{n,theo}}$ = 4100 g·mol^{-1}, $M_{\mathrm{n,NMR}}$ =5400 g·mol^{-1}, SEC(DMAc): $M_{\mathrm{n,SEC}}$ = 6400 g·mol^{-1}, $Đ$ = 1.06).

Synthesis of Double Adamantyl Endfunctionalized PDEA (Ad$_2$-PDEA$_{51}$)

CTA1 (54.0 mg, 0.07 mmol, 1.0 eq.), DEA (500.0 mg, 3.94 mmol, 55.6 eq.), AIBN (2.4 mg, 0.02 mmol, 0.2 eq.), DMF (3.3 mL) and a stirring-bar were added into a Schlenk-tube. After three freeze-pump-thaw cycles the tube was backfilled with argon, sealed, placed in an oil bath at 60 °C and removed after 24 h. The tube was subsequently cooled with liquid nitrogen to stop the reaction. A NMR-sample was withdrawn for the determination of conversion and $CDCl_3$ was added. A quantitative conversion was calculated based on the NMR data (see Characterization Methods for details of the calculation). The residue was dialysed against deionized water with a SpectraPor3 membrane (MWCO = 1000 Da) for 3 days at ambient temperature. The solvent was removed in vacuo to yield Ad$_2$-PDEA$_{51}$ as a yellow solid (0.45 g, 76%, $M_{\mathrm{n,theo}}$ = 7800 g·mol^{-1}, $M_{\mathrm{n,NMR}}$ = 7300 g·mol^{-1}, SEC(DMAc): $M_{\mathrm{n,SEC}}$ = 6800 g·mol^{-1}, $Đ$ = 1.11).

Synthesis of Mid-Chain Adamantyl-Functionalized PDMA (m-Ad-PDMA$_{114}$)

CTA2 (160.0 mg, 0.20 mmol, 1.0 eq.), DMA (2.00 g, 20.18 mmol, 100.9 eq.), AIBN (6.6 mg, 0.04 mmol, 0.2 eq.), DMF (18.0 mL) and a stirring-bar were added into a Schlenk-tube. After three freeze-pump-thaw cycles the tube was backfilled with argon, sealed, placed in an oil bath at 60 °C and removed after 6 h. The tube was subsequently cooled with liquid nitrogen to stop the reaction. A NMR-sample was withdrawn for the determination of conversion and $CDCl_3$ was added. A conversion of 88% was calculated based on the NMR data (see Characterization Methods for details of the calculation). The residue was dialysed against deionized water with a SpectraPor3 membrane (MWCO = 1000 Da) for 3 days at ambient temperature. The solvent was removed in vacuo to yield m-Ad-PDMA$_{114}$ as a yellow solid (0.74 g, 42%, $M_{\mathrm{n,theo}} = 9600\ \mathrm{g{\cdot}mol^{-1}}$, $M_{\mathrm{n,NMR}} = 12100\ \mathrm{g{\cdot}mol^{-1}}$, SEC(DMAc): $M_{\mathrm{n,SEC}} = 12000\ \mathrm{g{\cdot}mol^{-1}}$, $Đ = 1.10$).

Synthesis of Mid-Chain Adamantyl-Functionalized PDEA (m-Ad-PDEA$_{47}$)

CTA2 (250.0 mg, 0.32 mmol, 1.0 eq.), DEA (2.00 g, 15.75 mmol, 49.2 eq.), AIBN (10.3 mg, 0.06 mmol, 0.2 eq.), DMF (20.0 mL) and a stirring-bar were added into a Schlenk-tube. After three freeze-pump-thaw cycles the tube was backfilled with argon, sealed, placed in an oil bath at 60 °C and removed after 6 h. The tube was subsequently cooled with liquid nitrogen to stop the reaction. A NMR-sample was withdrawn for the determination of conversion and $CDCl_3$ was added. A conversion of 91% was calculated based on the NMR data (see Characterization Methods for details of the calculation). The residue was dialysed against deionized water with a SpectraPor3 membrane (MWCO = 1000 Da) for 3 days at ambient temperature. The solvent was removed in vacuo to yield m-Ad-PDEA$_{47}$ as a yellow solid (1.59 g, 87%, $M_{\mathrm{n,theo}} = 6500\ \mathrm{g{\cdot}mol^{-1}}$, $M_{\mathrm{n,NMR}} = 6800\ \mathrm{g{\cdot}mol^{-1}}$, SEC(DMAc): $M_{\mathrm{n,SEC}} = 5400\ \mathrm{g{\cdot}mol^{-1}}$, $Đ = 1.08$).

Synthesis of Mid-Chain Adamantyl-Functionalized P(DEA-b-DMA) (m-Ad-P(DEA_{47}-b-DMA_{33}))

Mid-chain adamantyl-functionalized PDEA (m-Ad-$PDEA_{47}$; $M_{n,NMR}$ = 6800 g·mol^{-1}; 800.0 mg, 0.12 mmol, 1.0 eq.), DMA (816.0 mg, 8.24 mmol, 68.7 eq.), AIBN (3.9 mg, 0.02 mmol, 0.2 eq.), DMF (10.6 mL) and a stirring-bar were added into a Schlenk-tube. After three freeze-pump-thaw cycles the tube was backfilled with argon, sealed, placed in an oil bath at 60 °C and removed after 6 h. The tube was subsequently cooled with liquid nitrogen to stop the reaction. The residue was dialysed against deionized water with a SpectraPor3 membrane (MWCO = 1000 Da) for 3 days at ambient temperature. The solvent was removed in vacuo to yield m-Ad-P(DEA_{47}-*b*-DMA_{33}) as a yellow solid (1.32 g, 82%, $M_{n,NMR}$ = 10800 g·mol^{-1}, SEC(DMAc): $M_{n,SEC}$ = 10400 g·mol^{-1}, $Đ$ = 1.13).

Synthesis of Mid-Chain Alkyne-Functionalized PDEA (m-alk-$PDMA_{90}$)

CTA3 (82.0 mg, 0.14 mmol, 1.0 eq.), DEA (2.80 g, 22.05 mmol, 157.5 eq.), AIBN (5.0 mg, 0.03 mmol, 0.2 eq.), DMF (7.0 mL) and a stirring-bar were added into a Schlenk-tube. After three freeze-pump-thaw cycles the tube was backfilled with argon, sealed, placed in an oil bath at 60 °C and removed after 1.5 h. The tube was subsequently cooled with liquid nitrogen to stop the reaction. The residue was dialysed against deionized water with a SpectraPor3 membrane (MWCO = 1000 Da) for 3 days at ambient temperature. The solvent was removed in vacuo to yield m-alk-$PDMA_{90}$ as a yellow solid (2.17 g, $M_{n,NMR}$ = 12000 g·mol^{-1}, SEC(DMAc): $M_{n,SEC}$ = 12400 g·mol^{-1}, $Đ$ = 1.15).

Synthesis of Mid-Chain Alkyne-Functionalized PDEA (m-alk-$PDMA_{39}$)

CTA3 (230.0 mg, 0.42 mmol, 1.0 eq.), DEA (2.00 g, 15.75 mmol, 37.5 eq.), AIBN (13.0 mg, 0.08 mmol, 0.2 eq.), DMF (10.0 mL) and a stirring-bar were added into a Schlenk-tube. After three freeze-pump-thaw cycles the tube was backfilled with argon, sealed, placed in an oil bath at 60 °C and removed after 3 h. The tube was subsequently cooled with liquid nitrogen to stop the reaction. A NMR-sample was withdrawn for the determination of conversion and $CDCl_3$ was added. A conversion of 63% was calculated based on the NMR data (see Characterization Methods for details of the calculation). The residue was dialysed against deionized water with a SpectraPor3 membrane (MWCO = 1000 Da) for 3 days at ambient temperature. The solvent was removed in vacuo to yield m-alk-PDMA$_{39}$ as a yellow solid (1.09 g, 55%, $M_{\mathrm{n,theo}}$ = 3600 g·mol^{-1}, $M_{\mathrm{n,NMR}}$ = 5500 g·mol^{-1}, SEC(DMAc): $M_{\mathrm{n,SEC}}$ = 3900 g·mol^{-1}, $Đ$ = 1.10).

Synthesis of Mid-Chain Alkyne-Functionalized P(DEA-b-DMA) (m-alk-P(DEA$_{39}$-b-DMA$_{37}$))

Mid-chain alkyne-functionalized PDEA$_{39}$ (m-alk-PDMA$_{39}$; $M_{\mathrm{n,NMR}}$ = 5500 g·mol^{-1}; 800.0 mg, 0.15 mmol, 1.0 eq.), DMA (1.10 g, 11.10 mmol, 76.3 eq.), AIBN (8.0 mg, 0.05 mmol, 0.3 eq.), DMF (6.4 mL) and a stirring-bar were added into a Schlenk-tube. After three freeze-pump-thaw cycles the tube was backfilled with argon, sealed, placed in an oil bath at 60 °C and removed after 3 h. The tube was subsequently cooled with liquid nitrogen to stop the reaction. The residue was dialysed against deionized water with a SpectraPor3 membrane (MWCO = 1000 Da) for 3 days at ambient temperature. The solvent was removed in vacuo to yield m-alk-P(DEA39-*b*-DMA37) as a yellow solid (1.33 g, 70%, $M_{\mathrm{n,NMR}}$ = 12500 g·mol^{-1}, SEC(DMAc): $M_{\mathrm{n,SEC}}$ = 9200 g·mol^{-1}, $Đ$ = 1.10).

ω-Endgroup Removal of Mid-Chain Alkyne-Functionalized m-alk-PDEA$_{90}$-OH

AIBN (0.55 g, 3.35 mmol, 41.9 eq.) was dissolved in unstabilized THF (80 mL) and heated to 60 °C under vigorous stirring. After 30 min a peroxide test confirmed successful peroxide formation and mid-chain alkyne-functionalized PDEA (m-alk-PDEA$_{90}$; $M_{\mathrm{n,NMR}}$ = 12000 g·mol^{-1}, 1.00 g, 0.08 mmol, 1.0 eq.) was added. The mixture was stirred at 60 °C until the yellow color vanished. L-(+)-Ascorbic acid (176.0 mg, 0.88 mmol, 11.1 eq.) was added and the mixture stirred at 60 °C for 30 min. Subsequently the mixture was cooled to ambient temperature and the solvent evaporated. The residue was dissolved in a mixture of THF and deionized H_2O, dialyzed against deionized H_2O for 3 days, filtered and lyophilized to yield m-alk-PDEA$_{90}$-OH as off-white solid (0.86 g, 86%).

ω-Endgroup Removal of Mid-Chain Alkyne-Functionalized P(DEA$_{39}$-b-DMA$_{37}$)-OH

AIBN (0.32 g, 1.95 mmol, 39.0 eq.) was dissolved in unstabilized THF (50 mL) and heated to 60 °C under vigorous stirring. After 30 min a peroxide test confirmed successful peroxide formation and mid-chain alkyne-functionalized P(DEA-*b*-DMA) (m-alk-P(DEA$_{39}$-*b*-DMA$_{37}$); $M_{n,NMR}$ = 12500 g·mol^{-1}, 0.60 g, 0.05 mmol, 1.0 eq.) was added. The mixture was stirred at 60 °C until the yellow color vanished. L-(+)-Ascorbic acid (100.0 mg, 0.51 mmol, 10.1 eq.) was added and the mixture stirred at 60 °C for 30 min. Subsequently the mixture was cooled to ambient temperature and the solvent evaporated. The residue was dissolved in a mixture of THF and deionized H_2O, dialyzed against deionized H_2O for 3 days, filtered and lyophilized to yield P(DEA$_{39}$-*b*-DMA$_{37}$)-OH as off-white solid (0.30 g, 51%).

Click-Reaction of Mid-Chain Alkyne-Functionalized PDEA with β-CD-N$_3$ (m-β-CD-PDEA$_{90}$)

Mid-chain alkyne functionalized PDEA$_{90}$ (m-alk-PDEA$_{90}$-OH; $M_{n,NMR}$ = 12000 g·mol^{-1}; 600.0 mg, 0.05 mmol, 1.0 eq.), β-CD-N$_3$ (594.0 mg, 0.51 mmol 10.3 eq.), PMDETA (157 µL, 0.75 mmol, 15.0 eq.), DMF (28.0 mL) and a stirring-bar were introduced into a Schlenk-tube. After three freeze-pump-thaw cycles the tube was filled with argon and CuBr (94.0 mg, 0.66 mmol, 13.1 eq.) was added under a stream of argon. Subsequently two freeze-pump-thaw cycles were performed, the tube backfilled with argon and the mixtures stirred at ambient temperature for 48 h. EDTA-solution (5 wt.%, 2 mL) was added and the residue was dialysed against deionized water with a SpectraPor3 membrane (MWCO = 2000 Da) for 3 days at ambient temperature. The solvent was removed in vacuo to yield the cyclodextrin functionalized polymer m-β-CD-PDEA$_{90}$ as off-white solid (571.0 mg, 86%, SEC(DMAc): $M_{\mathrm{n,SEC}}$ = 11100 g·mol^{-1}, $Đ$ = 1.30).

Click-Reaction of Mid-Chain Alkyne-Functionalized P(DEA-b-DMA) with β-CD-N$_3$ (m-β-CD-P(DEA$_{39}$-b-DMA$_{37}$))

Mid-chain alkyne functionalized P(DEA-*b*-DMA) (m-alk-P(DEA$_{39}$-*b*-DMA$_{37}$)-OH; $M_{\mathrm{n,NMR}}$ = 12500 g·mol^{-1}; 200.0 mg, 0.02 mmol, 1.0 eq.), β-CD-N$_3$ (190.0 mg, 0.16 mmol 8.0 eq.), PMDETA (50 µL, 0.24 mmol, 12.0 eq.), DMF (9.0 mL) and a stirring-bar were introduced into a Schlenk-tube. After three freeze-pump-thaw cycles the tube was filled with argon and CuBr (30.0 mg, 0.21 mmol, 10.5 eq.) was added under a stream of argon. Subsequently two freeze-pump-thaw cycles were performed, the tube backfilled with argon and the mixtures stirred at ambient temperature for 48 h. EDTA-solution (5 wt. %, 1 mL) was added and the residue was dialysed against deionized water with a SpectraPor3 membrane (MWCO = 2000 Da) for 3 days at ambient temperature. The solvent was removed in vacuo to yield the cyclodextrin functionalized polymer m-β-CD-P(DEA$_{39}$-*b*-DMA$_{37}$) as off-white solid (210.0 mg, 77%, SEC(DMAc): $M_{\mathrm{n,SEC}}$ = 7600 g·mol^{-1}, $Đ$ = 1.26).

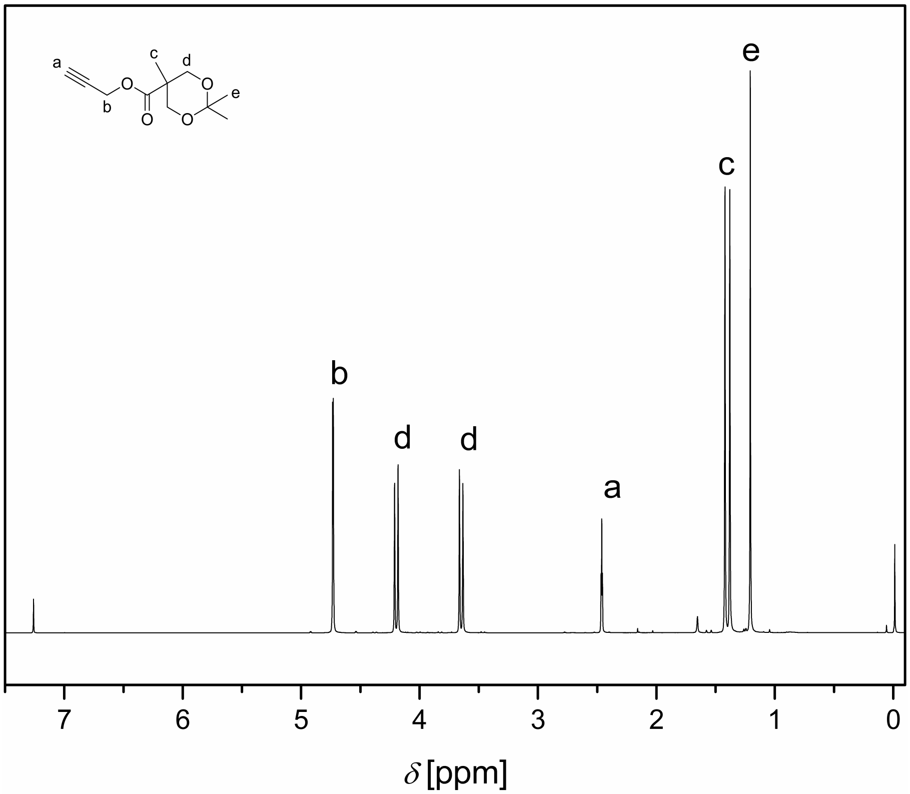

Figure S1. ^{1}H-NMR spectrum of prop-2-yn-1-yl 2,2,5-trimethyl-1,3-dioxane-5-carboxylate recorded in $CDCl_3$ at 400 MHz.

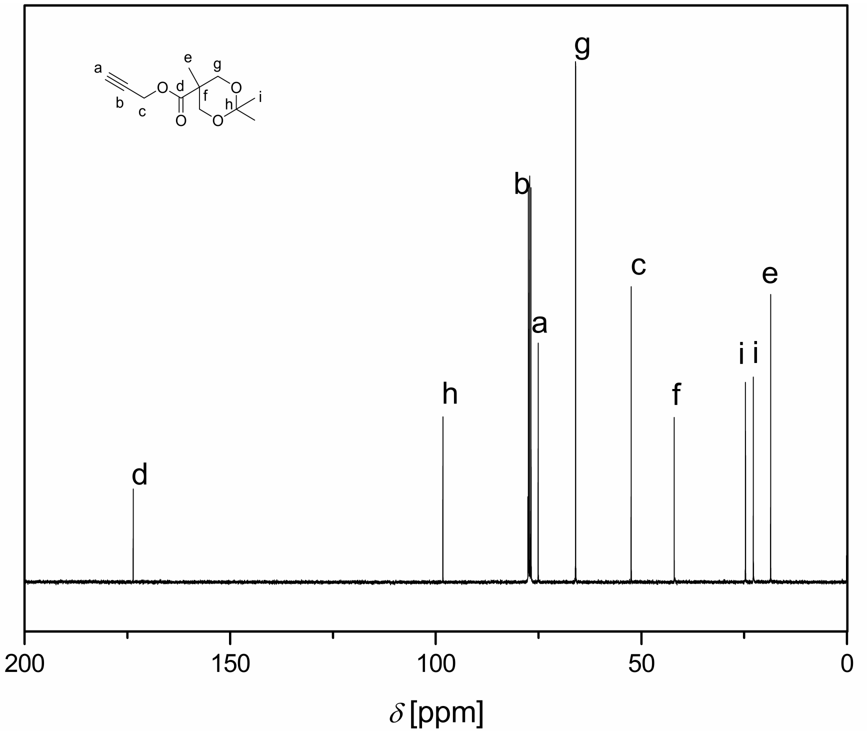

Figure S2. ^{13}C-NMR spectrum of prop-2-yn-1-yl 2,2,5-trimethyl-1,3-dioxane-5-carboxylate recorded in $CDCl_3$ at 100 MHz.

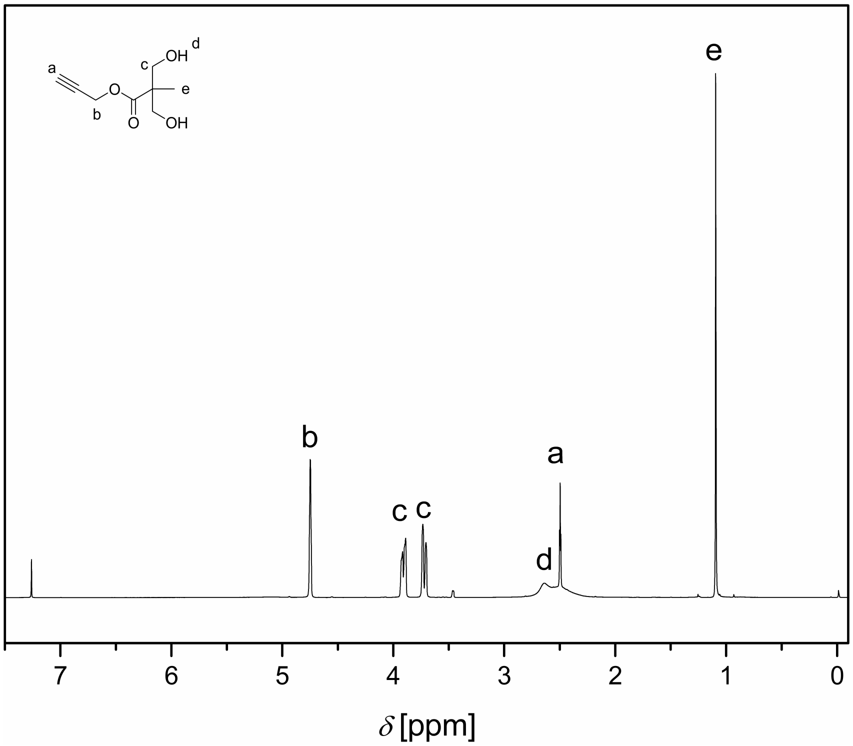

Figure S3. ^{1}H-NMR spectrum of prop-2-yn-1-yl 3-hydroxy-2-(hydroxymethyl)-2-methylpropanoate recorded in $CDCl_3$ at 400 MHz.

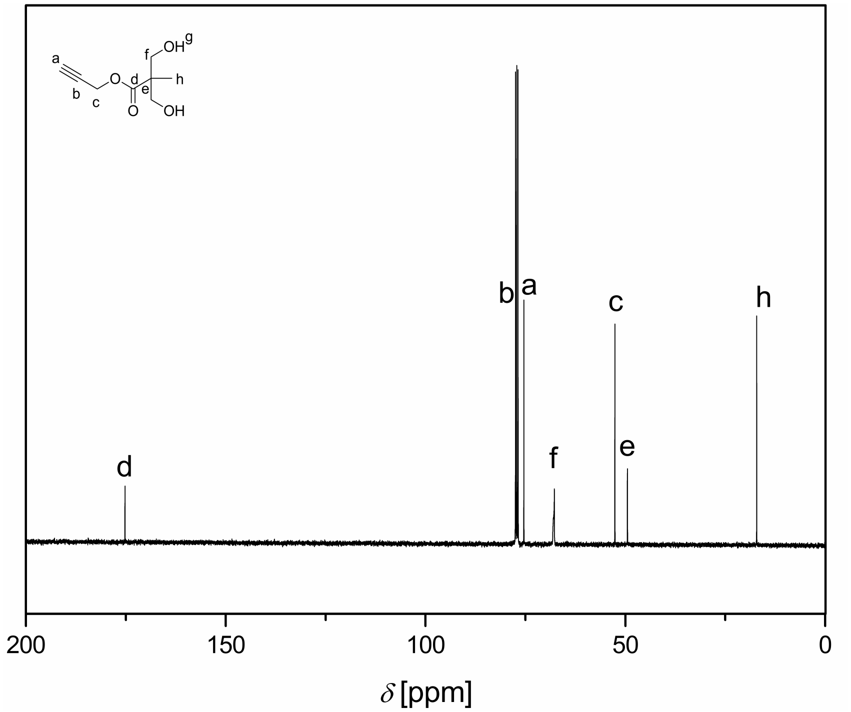

Figure S4. ^{13}C-NMR spectrum of prop-2-yn-1-yl 3-hydroxy-2-(hydroxymethyl)-2-methylpropanoate recorded in $CDCl_3$ at 100 MHz.

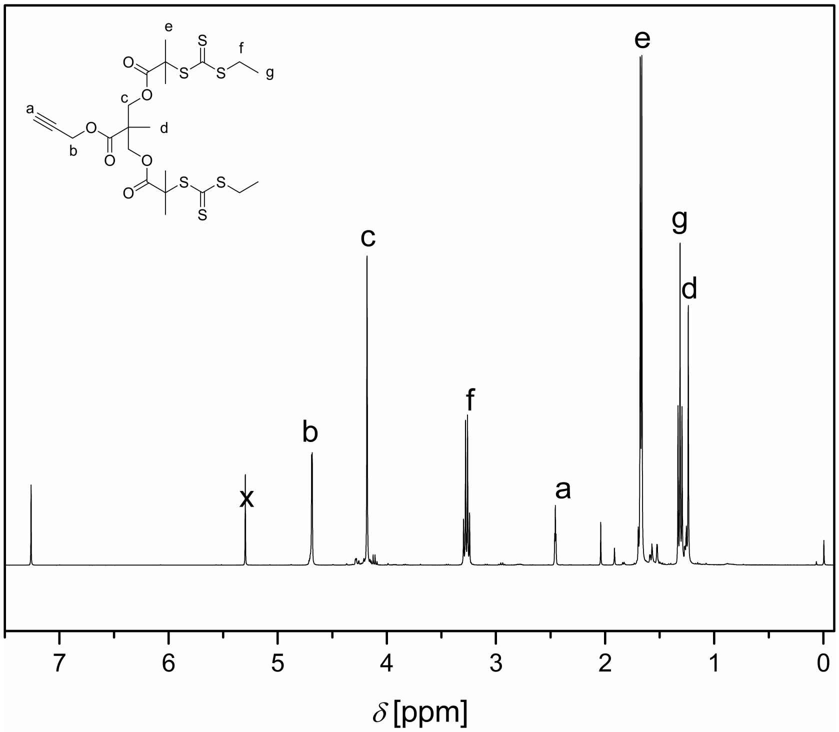

Figure S5. ^{1}H-NMR spectrum of 2-methyl-2-((prop-2-yn-1-yloxy)carbonyl)propane-1,3-diyl bis(2-(((ethylthio)carbonothioyl)thio)-2-methylpropanoate) (**CTA3**) recorded in $CDCl_3$ at 400 MHz.

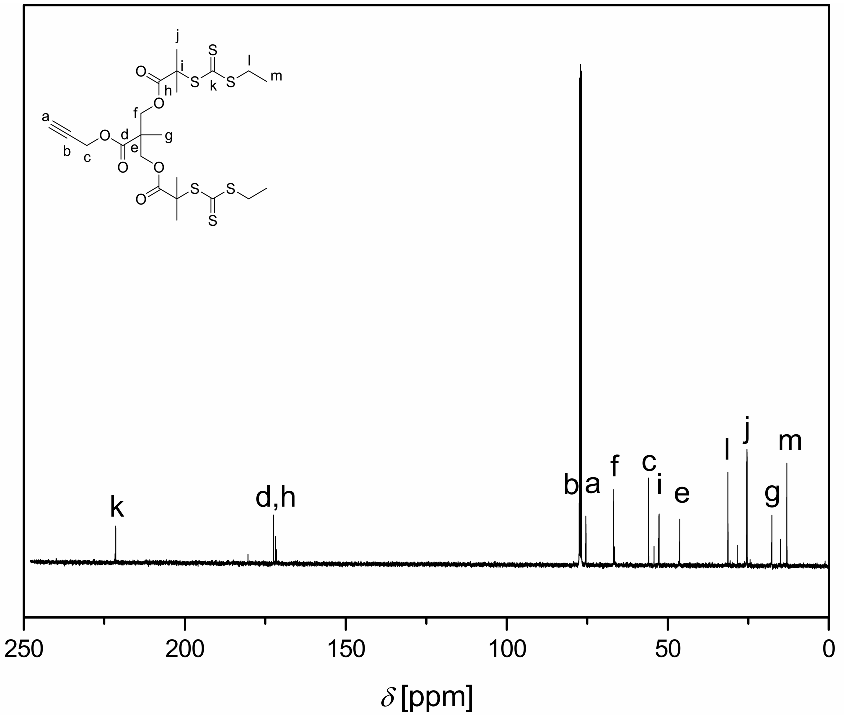

Figure S6. ^{13}C-NMR spectrum of 2-methyl-2-((prop-2-yn-1-yloxy)carbonyl)propane-1,3-diyl bis(2-(((ethylthio)carbonothioyl)thio)-2-methylpropanoate) (**CTA3**) recorded in $CDCl_3$ at 100 MHz.

Table S1. Results for the RAFT polymerization of DMA at 60 °C in DMF.

DMA/CTA/I	*t* / h	*Conv.* / %	$M_{n,theo}$ / g·mol^{-1}	$M_{n,NMR}$ / g·mol^{-1}	$M_{n,SEC}$ / g·mol^{-1}	*Đ*	Dp	label
CTA1 34/1/0.2	24	> 99	4100	5400	6400	1.06	57	Ad_2-$PDMA_{57}$
CTA2 101/1/0.2	6	88	9600	12100	12000	1.10	114	m-Ad-$PDMA_{114}$
CTA3 203/1/0.2	1	-	-	10900	10600	1.10	104	m-alk-$PDMA_{104}$

Table S2. Results for the RAFT polymerization of DEA at 60 °C in DMF.

DEA/CTA/I	*t* / h	*Conv.* / %	$M_{n,theo}$ / g·mol^{-1}	$M_{n,NMR}$ / g·mol^{-1}	$M_{n,SEC}$ / g·mol^{-1}	*Đ*	Dp	label
CTA1 56/1/0.2	24	> 99	7800	7300	6800	1.11	51	Ad_2-$PDEA_{51}$
CTA2 49/1/0.2	6	91	6500	6800	5400	1.08	47	m-Ad-$PDEA_{47}$
CTA3 158/1/0.2	1.5	-	-	12000	12400	1.15	90	m-alk-$PDEA_{90}$
CTA3 38/1/0.2	3	63	3600	5500	3900	1.10	39	m-alk-$PDEA_{39}$

Table S3. Results for the RAFT block copolymerization of DMA at 60 °C in DMF.

DMA/CTA/I	*t* / h	$M_{n,NMR}$ / g·mol^{-1}	$M_{n,SEC}$ / g·mol^{-1}	*Đ*	Dp	label
m-Ad-$PDEA_{47}$ 56/1/0.2	6	10800	10400	1.13	47+33	m-Ad-P(DEA_{47}-*b*-DMA_{33})
m-alk-$PDEA_{39}$ 38/1/0.2	3	12500	9300	1.10	39+37	m-alk-P(DEA_{39}-*b*-DMA_{37})

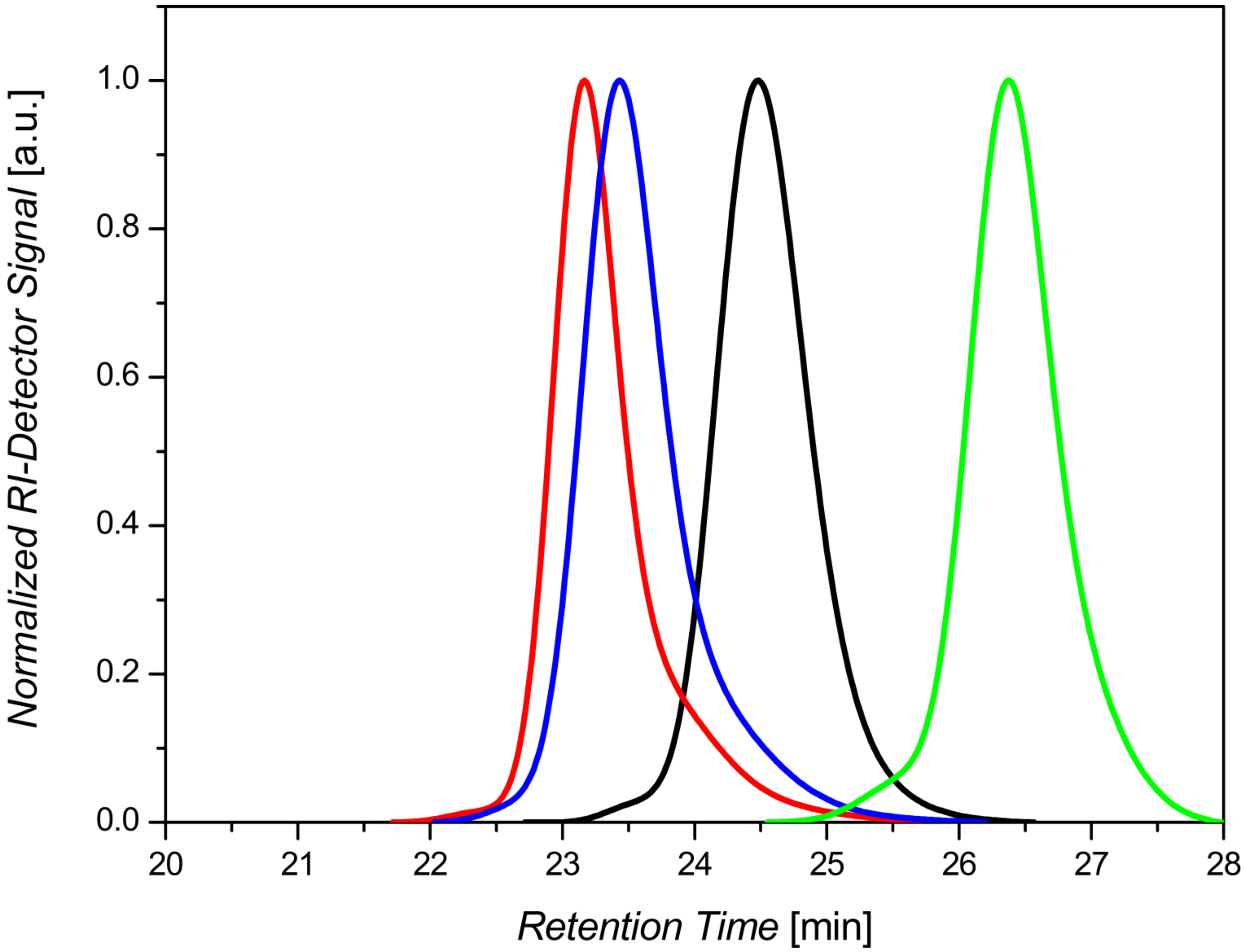

Figure S7. SEC traces of Ad$_2$-PDMA$_{57}$ (black, $M_{\mathrm{n,SEC}}$ = 6400 g·mol$^{-1,}$ $Đ$ = 1.06), m-Ad-PDMA$_{114}$ (red, $M_{\mathrm{n,SEC}}$ = 12000 g·mol$^{-1,}$ $Đ$ = 1.10), m-alk-PDMA$_{104}$ (blue, $M_{\mathrm{n,SEC}}$ = 10600 g·mol$^{-1,}$ $Đ$ = 1.10) and short chain m-alk-PDMA (green, $M_{\mathrm{n,SEC}}$ = 2000 g·mol$^{-1,}$ $Đ$ = 1.11) for ESI-MS measured in DMAc.

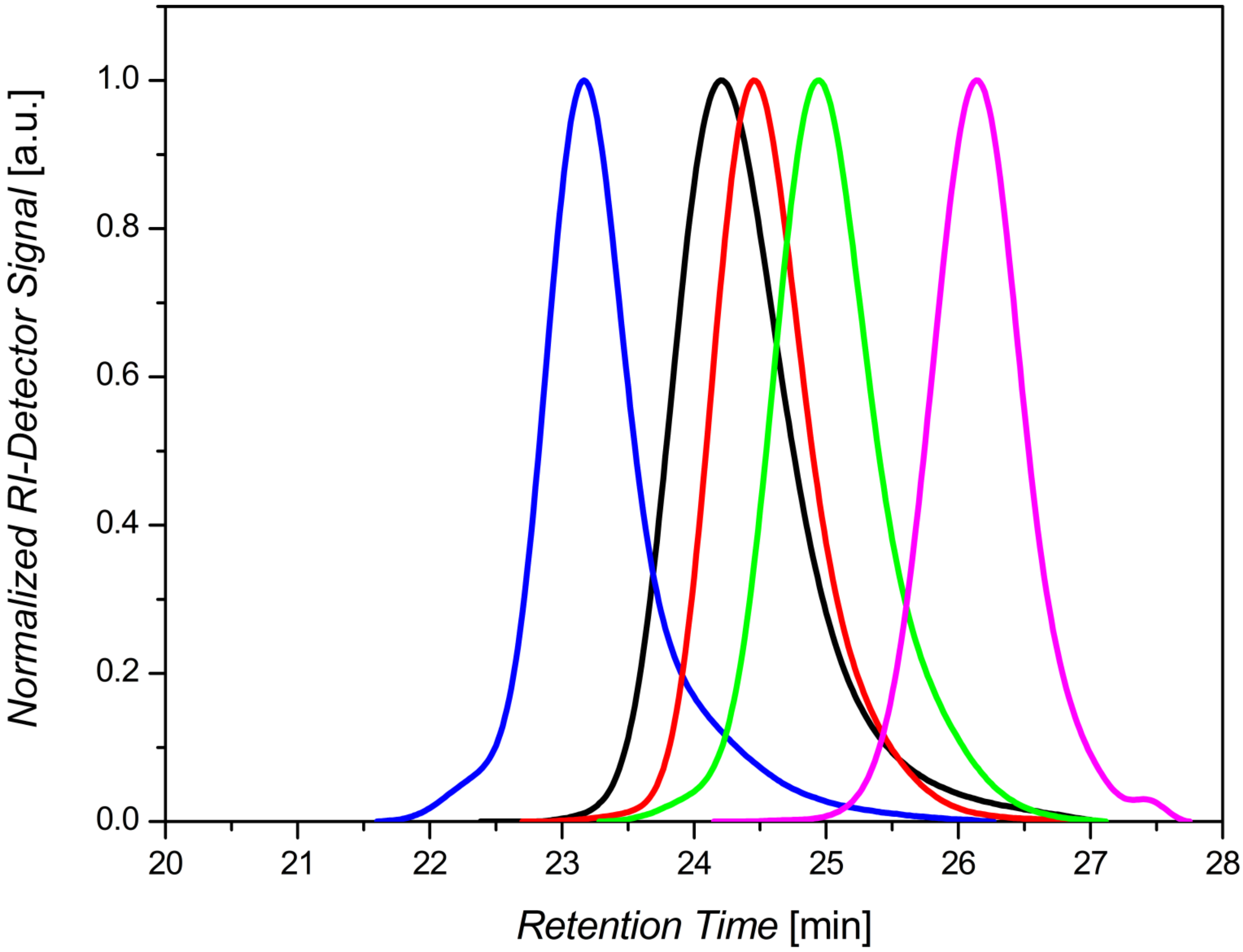

Figure S8. SEC traces of Ad_2-$PDEA_{51}$ (black, $M_{n,SEC}$ = 6800 g·mol$^{-1,}$ $Đ$ = 1.11), m-Ad-$PDEA_{47}$ (red, $M_{n,SEC}$ = 5400 g·mol$^{-1,}$ $Đ$ = 1.08), m-alk-$PDEA_{90}$ (blue, $M_{n,SEC}$ = 12400 g·mol$^{-1,}$ $Đ$ = 1.15), m-alk-$PDEA_{39}$ (green, $M_{n,SEC}$ = 3900 g·mol$^{-1,}$ $Đ$ = 1.10) and short chain m-alk-PDEA for ESI-MS (green, $M_{n,SEC}$ = 1800 g·mol$^{-1,}$ $Đ$ = 1.08) measured in DMAc.

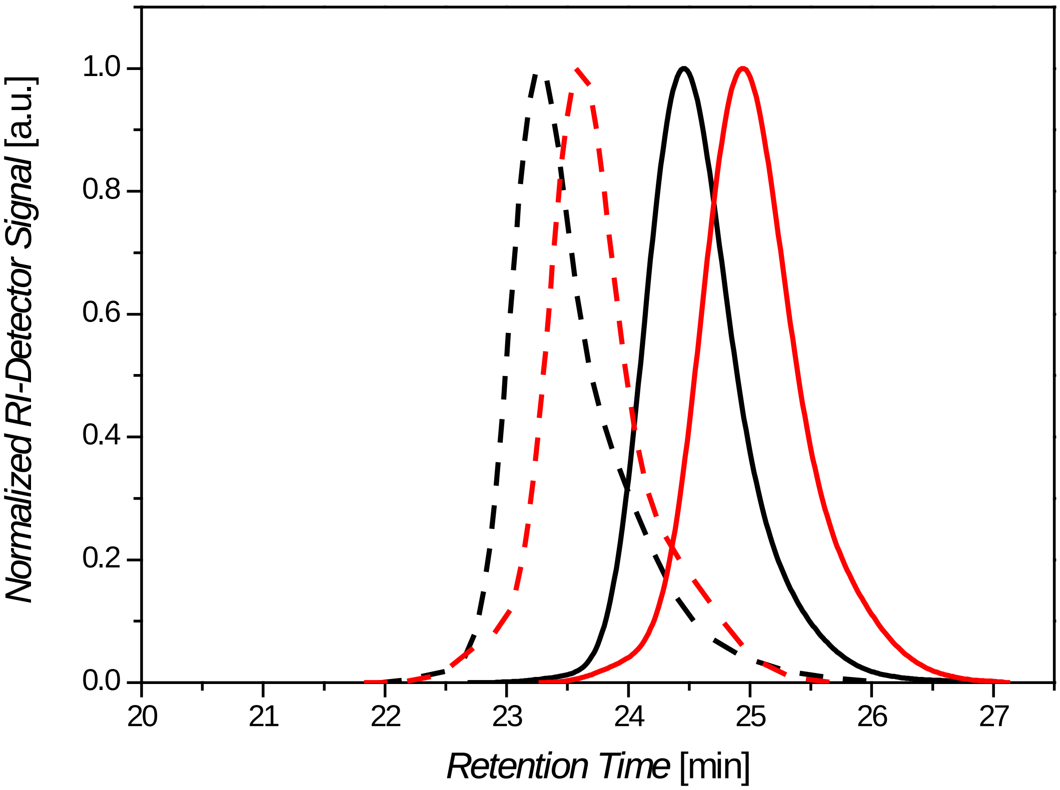

Figure S9. SEC traces of the block copolymers and their respective macro-CTAs: m-Ad-PDEA$_{47}$ (black, $M_{\mathrm{n,SEC}}$ = 5400 g·mol$^{-1,}$ $Đ$ = 1.08), m-Ad-P(DEA$_{47}$-*b*-DMA$_{33}$) (black dashed, $M_{\mathrm{n,SEC}}$ = 10400 g·mol$^{-1,}$ $Đ$ = 1.13), m-alk-PDEA$_{39}$ (red, $M_{\mathrm{n,SEC}}$ = 3900 g·mol$^{-1,}$ $Đ$ = 1.10) and m-alk-P(DEA$_{39}$-*b*-DMA$_{37}$) (red dashed, $M_{\mathrm{n,SEC}}$ = 9300 g·mol$^{-1,}$ $Đ$ = 1.10) measured in DMAc.

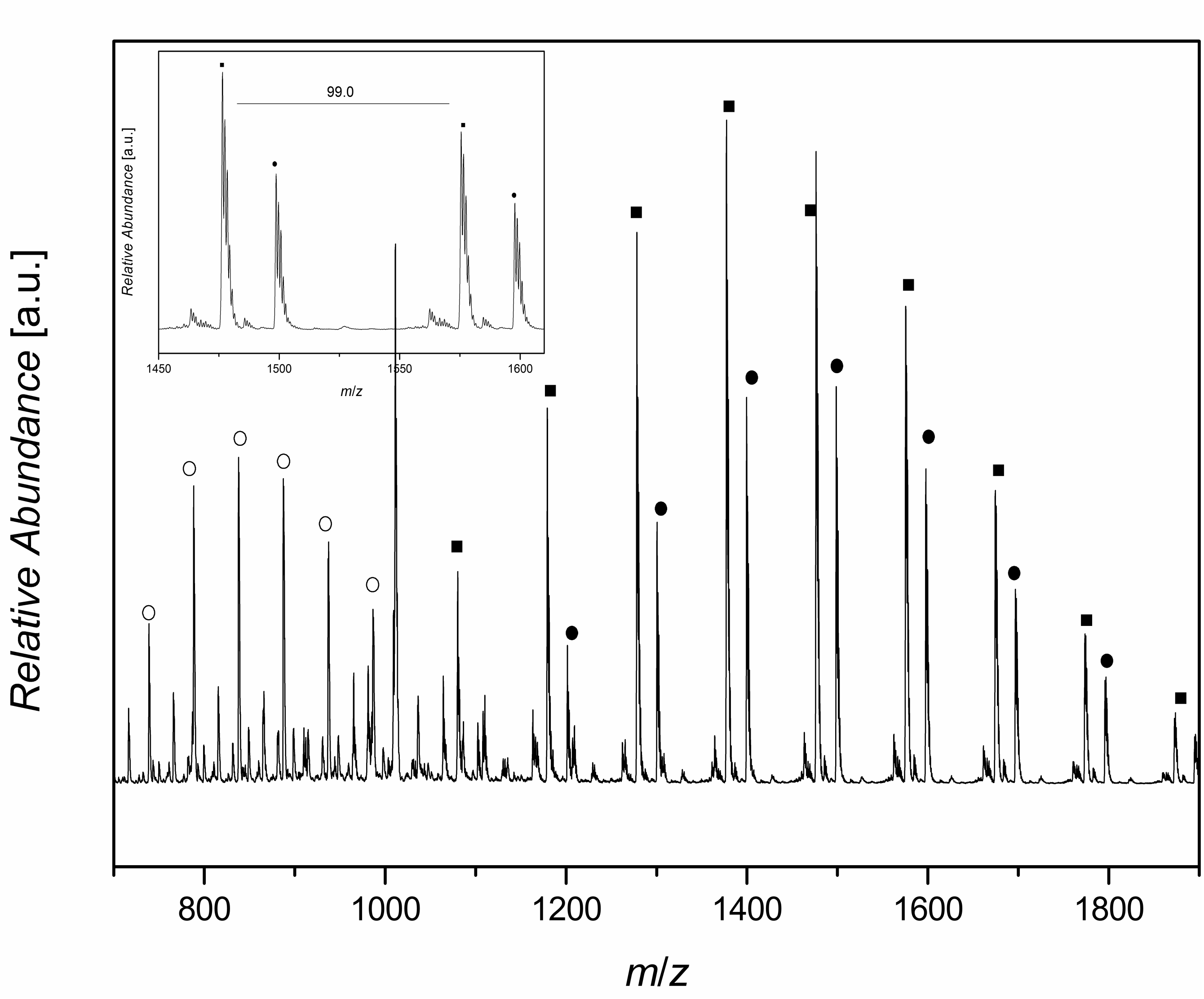

Figure S10. ESI-MS-spectrum of a mid-chain alkyne-functionalized PDMA ($M_{n,SEC} = 2000$ g·mol^{-1}, $Đ = 1.11$) polymerized with **CTA3**.

Table S4. Theoretical and experimental *m*/*z* of PDMA polymerized with **CTA3**.

Species	m/z_{theo}	$m/z_{exp.}$	$\Delta m/z$
■ [**CTA3**$(DMA)_9$+H]$^+$	1476.68	1476.50	0.18
● [**CTA3**$(DMA)_{23}$+Na]$^+$	1498.66	1498.75	0.09
○ [**CTA3**$(DMA)_{25}$+2H]$^{2+}$	887.44	887.42	0.02

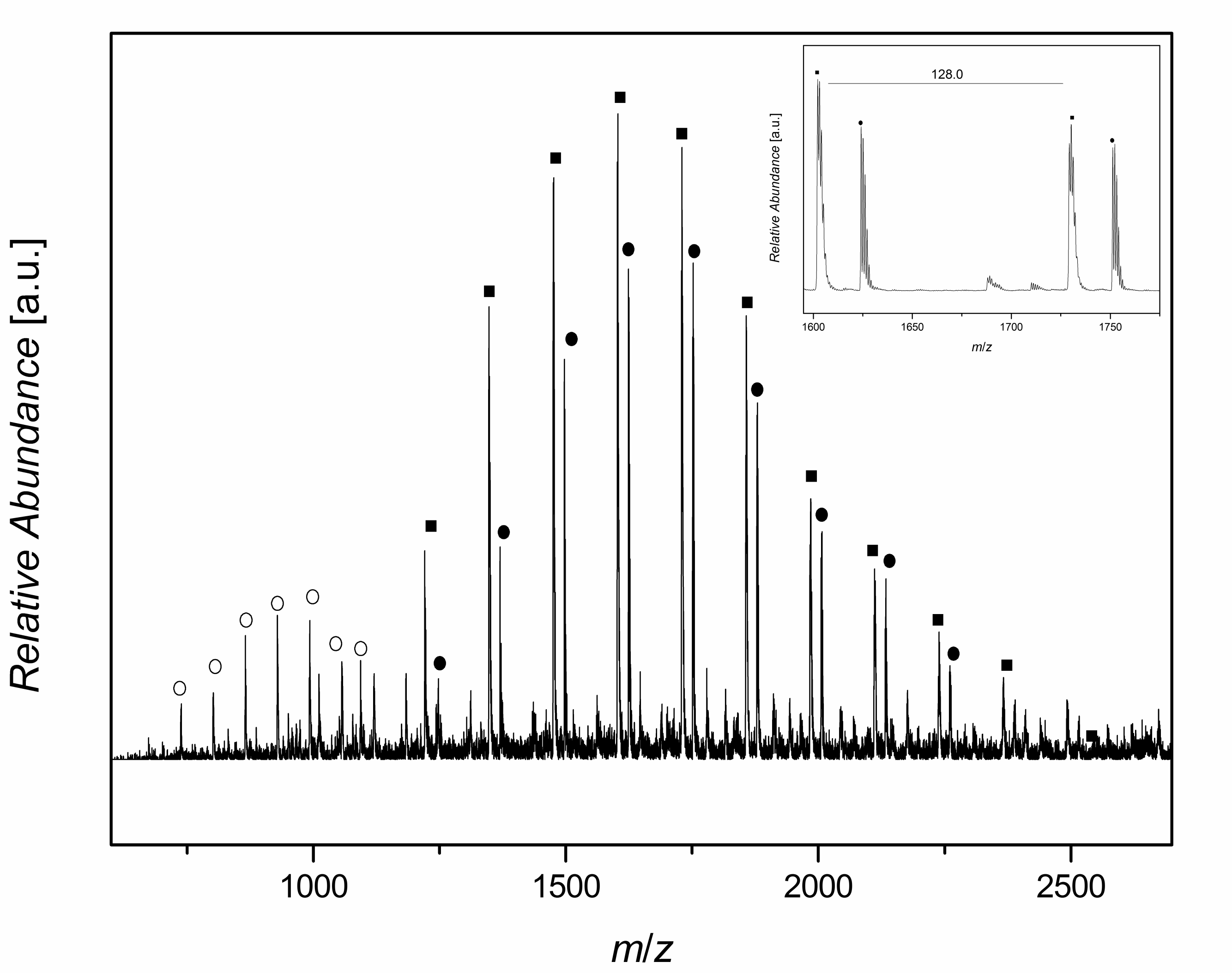

Figure S11. ESI-MS-spectrum of a mid-chain alkyne-functionalized PDEA ($M_{n,SEC} = 1800$ g·mol^{-1}, *Đ* = 1.08) polymerized with **CTA3**.

Table S5. Theoretical and experimental *m*/*z* of PDEA polymerized with **CTA3**.

Species	m/z_{theo}	$m/z_{exp.}$	$\Delta m/z$
■ [**CTA3**$(DEA)_8$+H]$^+$	1601.86	1602.09	0.23
● [**CTA3**$(DEA)_8$+Na]$^+$	1623.84	1624.09	0.25
○ [**CTA3**$(DEA)_{10}$+2H]$^{2+}$	928.53	929.09	0.56

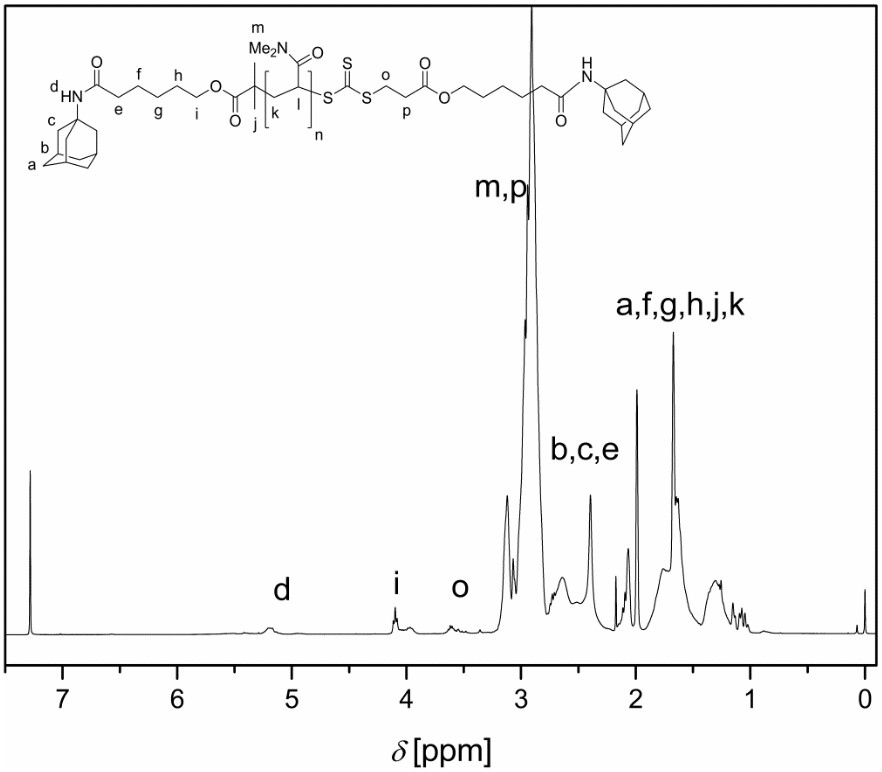

Figure S12. ^{1}H-NMR spectrum of double adamantyl-functionalized Ad$_2$-PDMA$_{57}$ ($M_{n,SEC}$ = 6400 g·mol^{-1}, $Đ$ = 1.06) recorded in CDCl$_3$ at 25 °C.

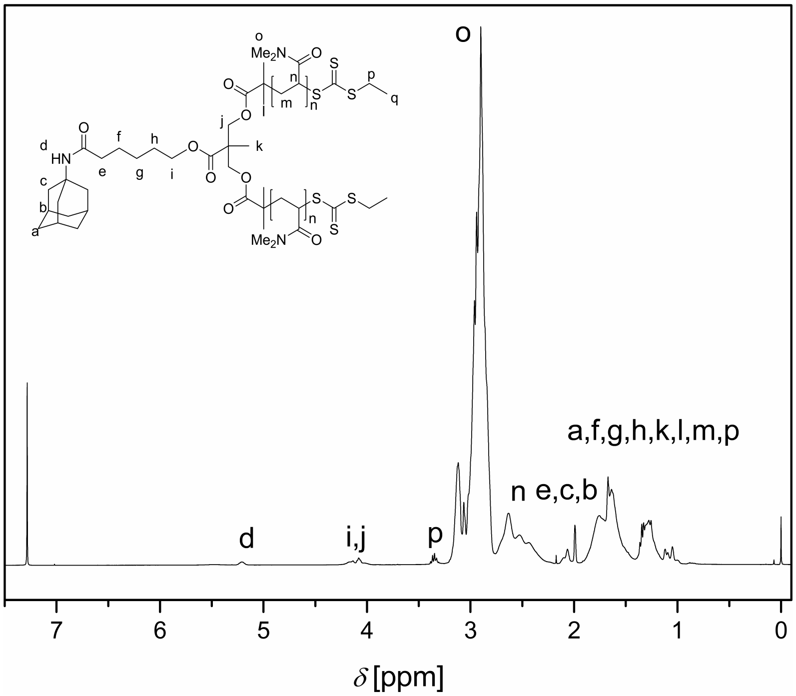

Figure S13. ^{1}H-NMR spectrum of mid-chain adamantyl-functionalized m-Ad-PDMA$_{114}$ ($M_{n,SEC}$ = 12100 g·mol^{-1}, $Đ$ = 1.10) recorded in CDCl$_3$ at 25 °C.

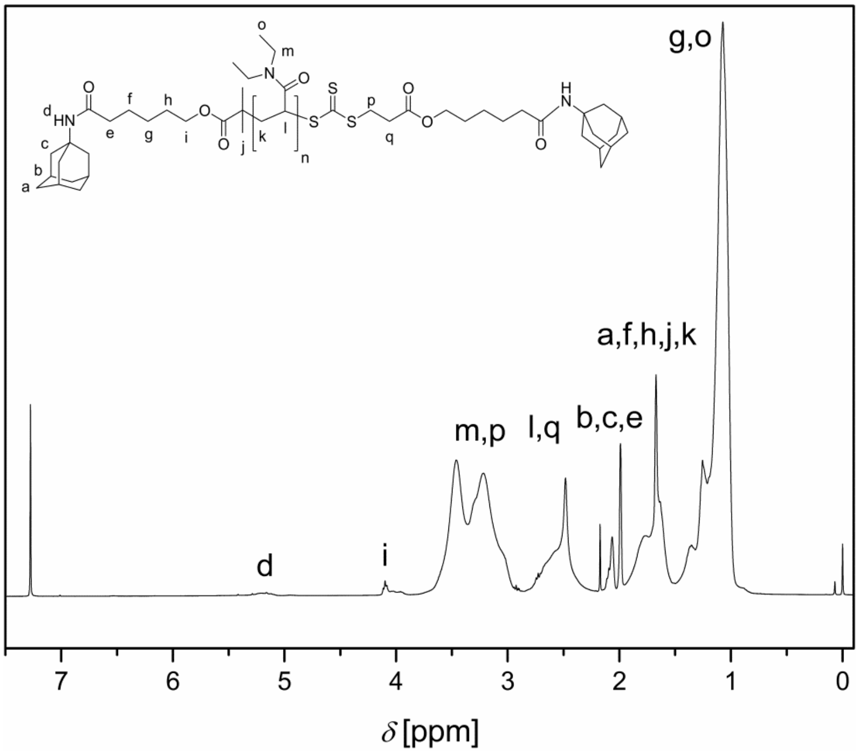

Figure S14. ^{1}H-NMR spectrum of double adamantyl-functionalized Ad$_2$-PDEA$_{51}$ ($M_{n,SEC}$=6800 g·mol^{-1}, $Đ$ = 1.11) recorded in CDCl$_3$ at 25 °C.

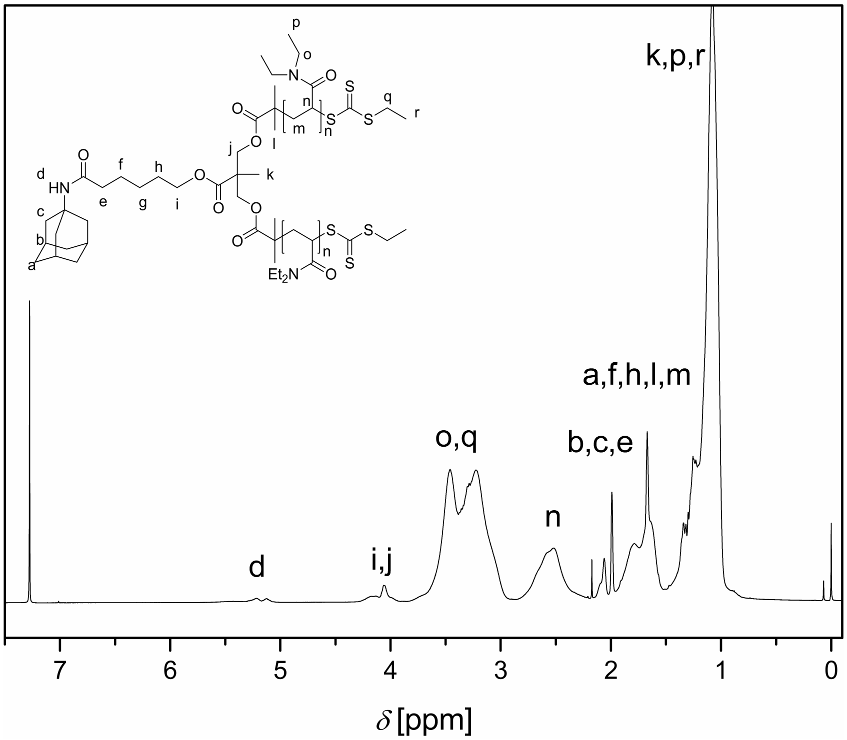

Figure S15. ^{1}H-NMR spectrum of mid-chain adamantyl-functionalized m-Ad-PDEA$_{47}$ ($M_{n,SEC}$ = 5400 g·mol^{-1}, $Đ$ = 1.08) recorded in CDCl$_3$ at 25 °C.

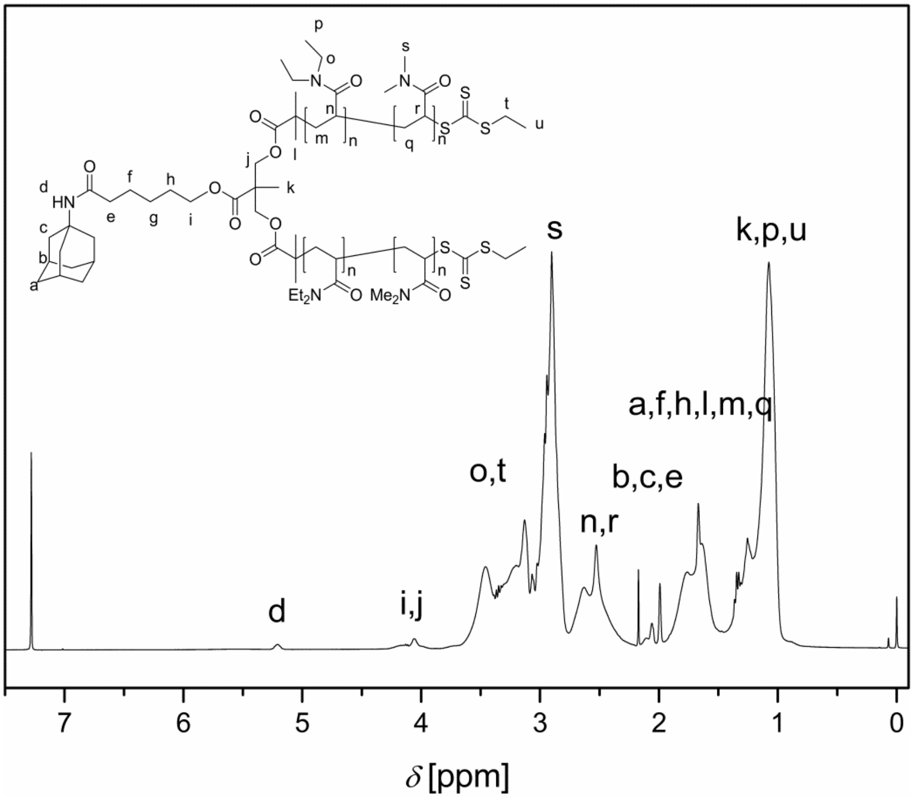

Figure S16. ^{1}H-NMR spectrum of mid-chain adamantyl-functionalized m-Ad-P(DEA$_{47}$-*b*-DMA$_{33}$) ($M_{n,SEC}$ = 10400 g·mol^{-1}, $Đ$ = 1.13) recorded in CDCl$_3$ at 25 °C.

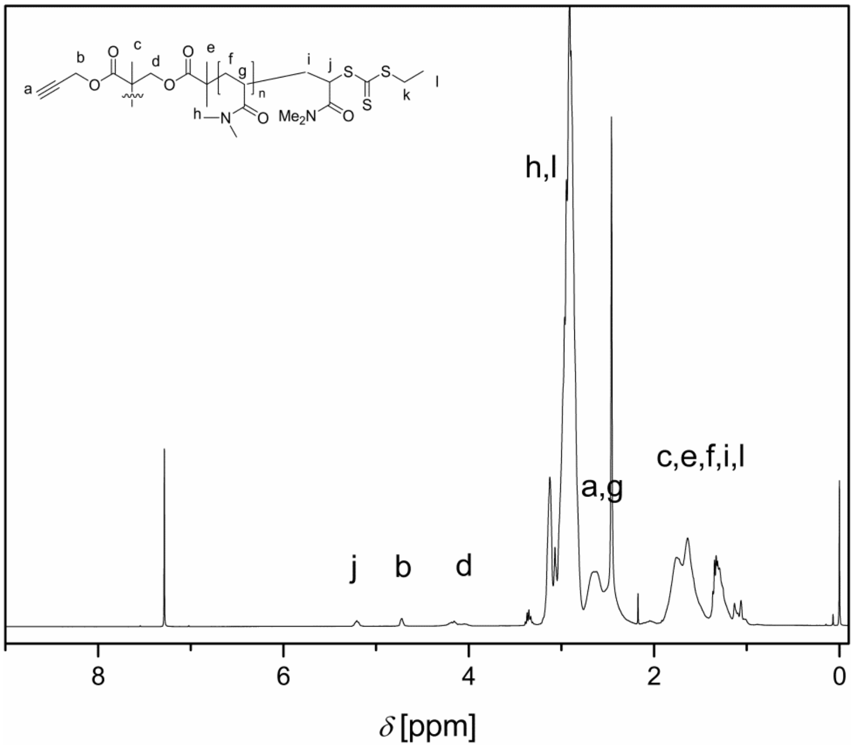

Figure S17. ^{1}H-NMR spectrum of mid-chain alkyne-functionalized m-alk-PDMA$_{104}$ ($M_{n,SEC}$ = 10600 g·mol^{-1}, $Đ$ = 1.10) recorded in CDCl$_3$ at 25 °C.

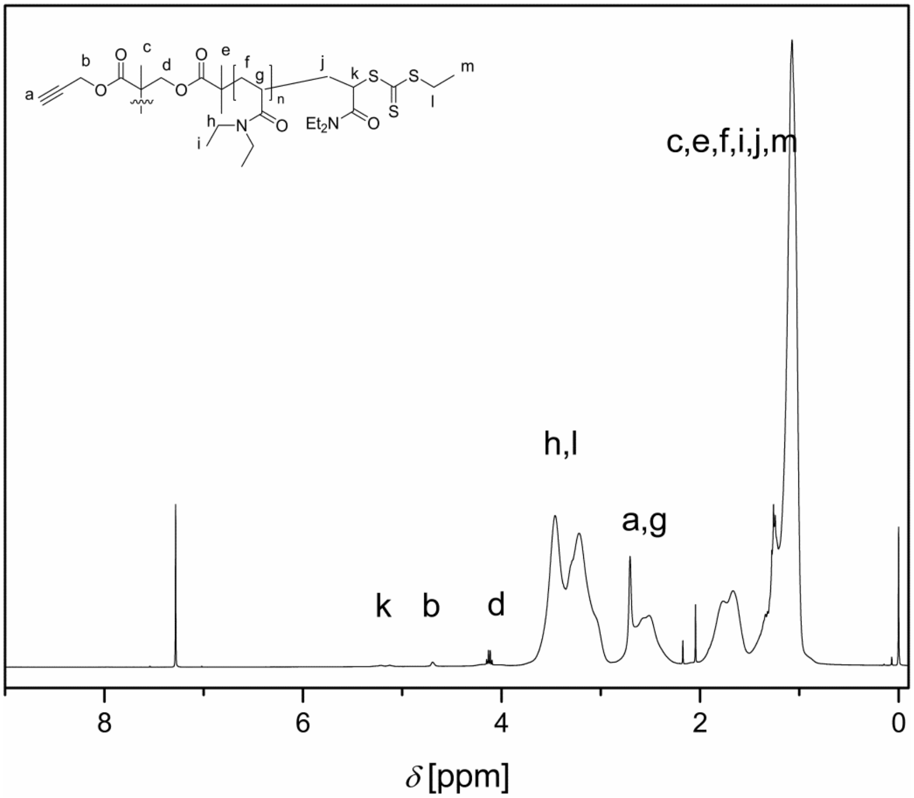

Figure S18. ^{1}H-NMR spectrum of mid-chain alkyne-functionalized m-alk-PDEA$_{90}$ ($M_{n,SEC}$ = 12400 g·mol^{-1}, $Đ$ = 1.15) recorded in CDCl$_3$ at 25 °C.

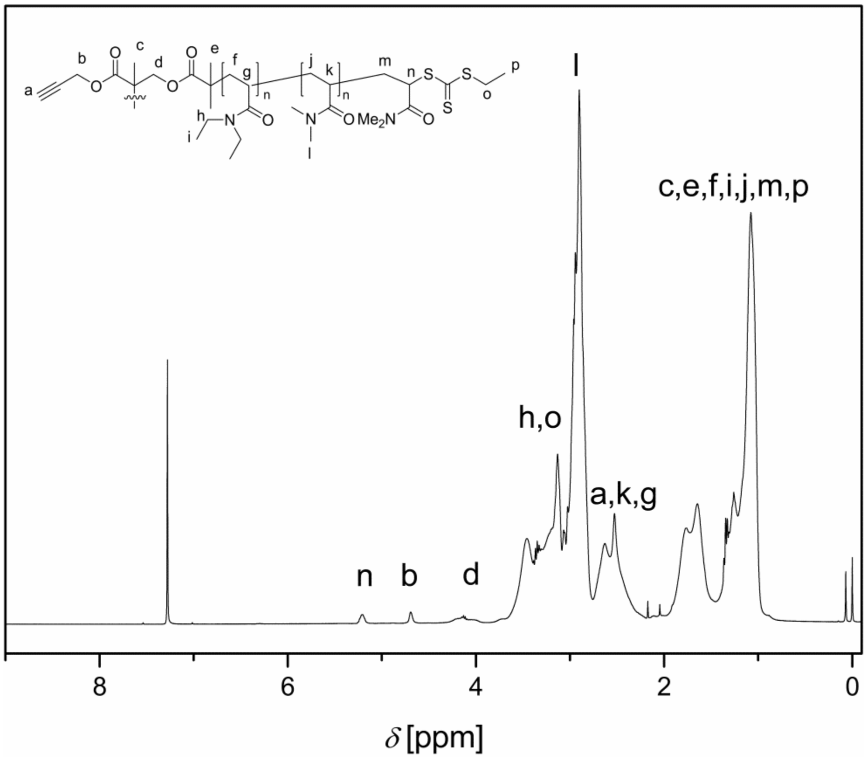

Figure S19. ^{1}H-NMR spectrum of mid-chain alkyne-functionalized m-alk-P(DEA$_{39}$-*b*-DMA$_{37}$) ($M_{n,SEC}$ = 9300 g·mol^{-1}, $Đ$ = 1.10) recorded in CDCl$_3$ at 25 °C.

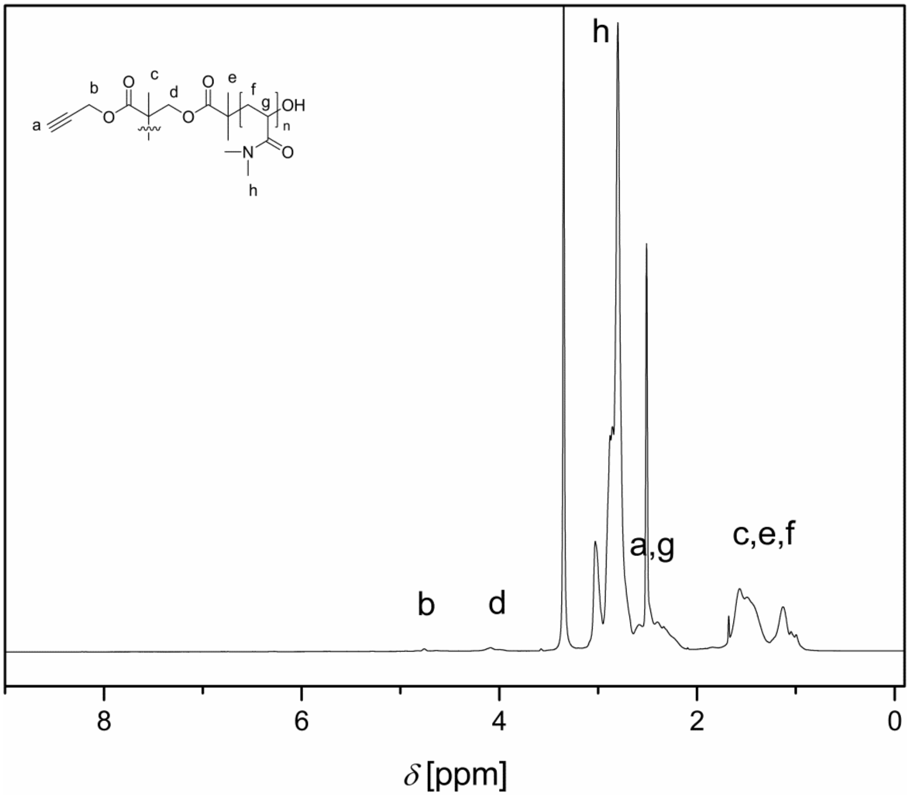

Figure S20. ^{1}H-NMR spectrum of mid-chain alkyne-functionalized m-alk-PDMA$_{104}$-OH after RAFT endgroup removal ($M_{n,SEC}$ = 10600 g·mol^{-1}, $Đ$ = 1.10) recorded in DMSO-d$_6$ at 25 °C.

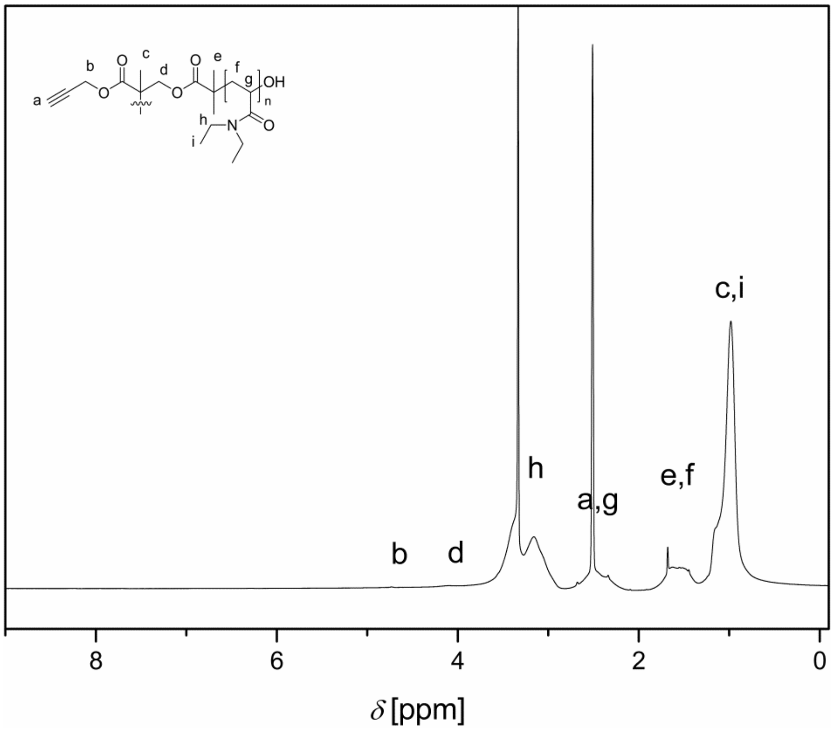

Figure S21. ^{1}H-NMR spectrum of mid-chain alkyne-functionalized m-alk-PDEA$_{90}$-OH after RAFT endgroup removal ($M_{n,SEC}$ = 12400 g·mol^{-1}, $Đ$ = 1.15) recorded in DMSO-d$_6$ at 25 °C.

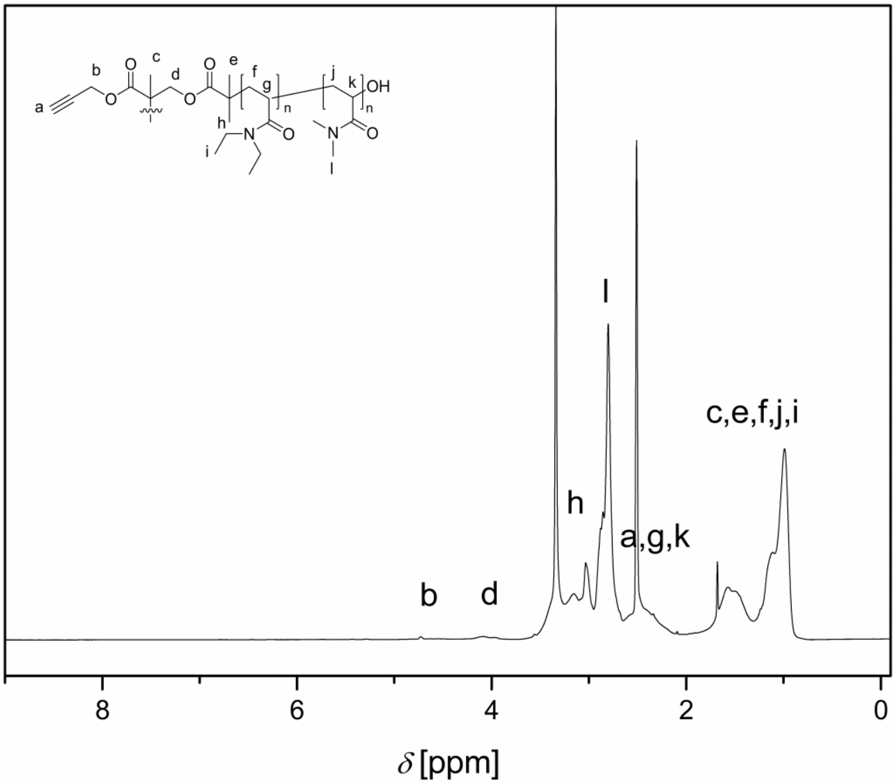

Figure S22. ^{1}H-NMR spectrum of mid-chain alkyne-functionalized m-alk-P(DEA$_{39}$-*b*-DMA$_{37}$)-OH after RAFT endgroup removal ($M_{\mathrm{n,SEC}}$ = 10200 g·mol^{-1}, $Đ$ = 1.26) recorded in DMSO-d$_6$ at 25 °C.

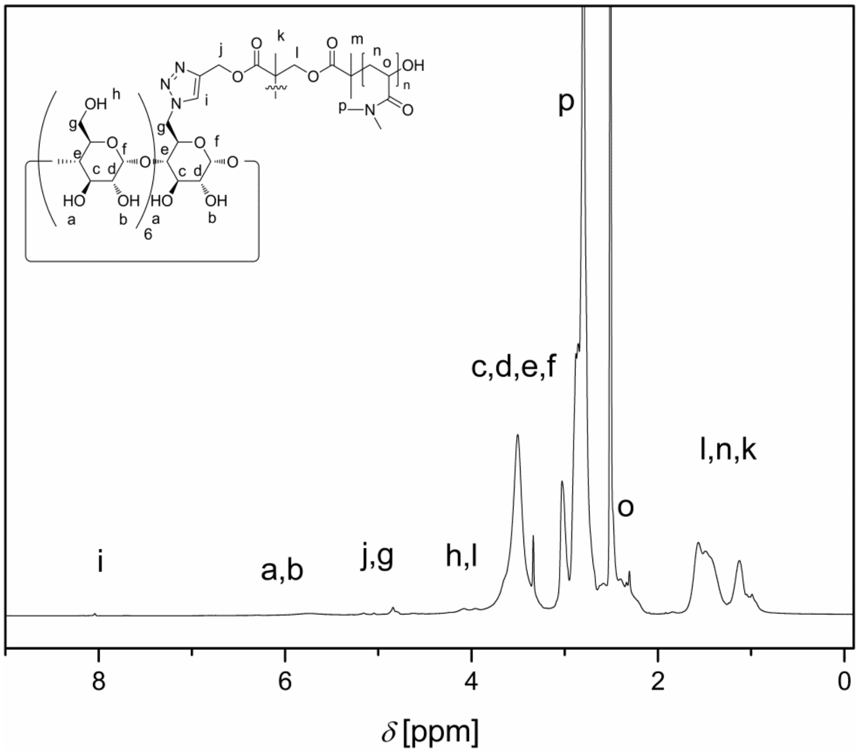

Figure S23. ^{1}H-NMR spectrum of mid-chain β-CD-functionalized m-β-CD-PDMA$_{104}$ ($M_{\mathrm{n,SEC}}$ = 10600 g·mol^{-1}, $Đ$ = 1.10) recorded in DMSO-d$_6$ at 25 °C.

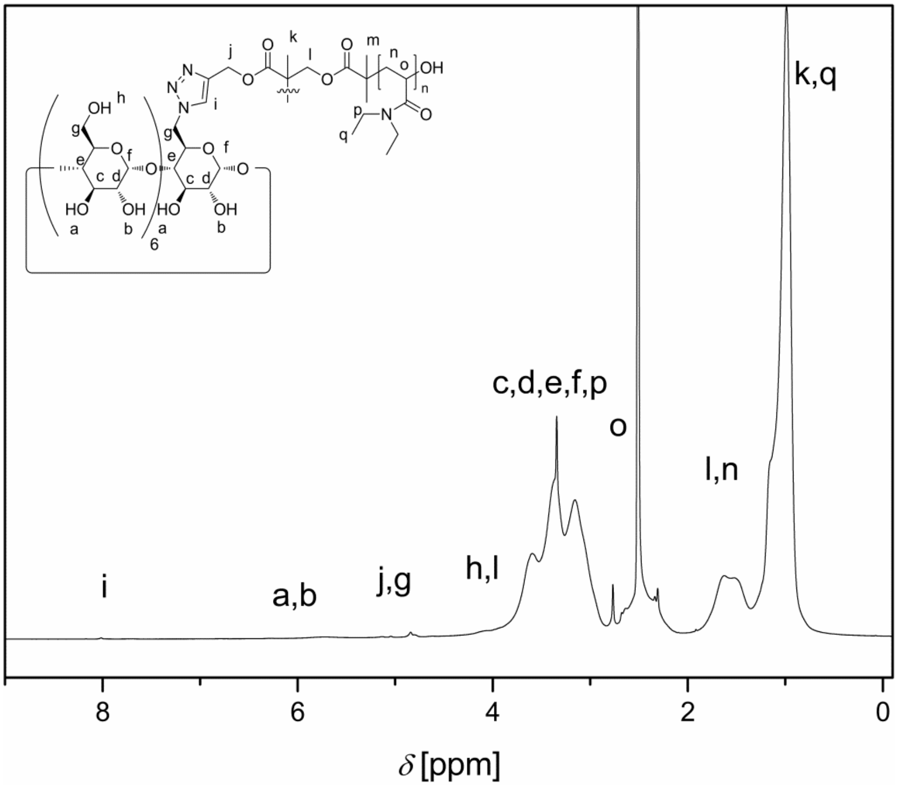

Figure S24. ^{1}H-NMR spectrum of mid-chain β-CD-functionalized m-β-CD-PDEA$_{90}$ ($M_{n,SEC}$ = 11200 g·mol^{-1}, $Đ$ = 1.30) recorded in DMSO-d$_6$ at 25 °C.

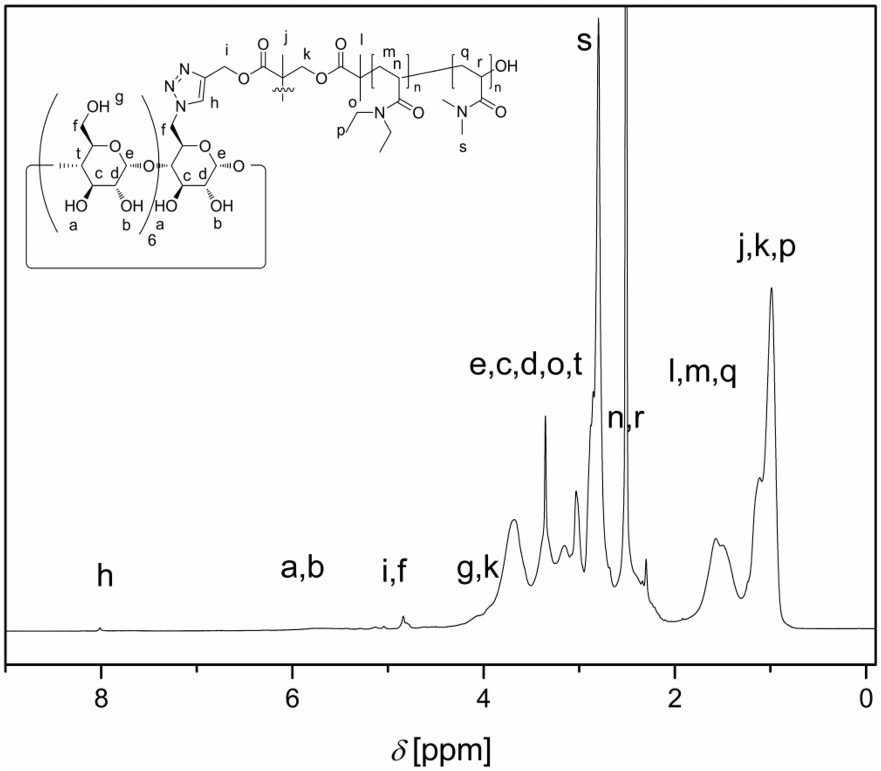

Figure S25. ^{1}H-NMR spectrum of mid-chain β-CD-functionalized m-β-CD-P(DEA$_{39}$-*b*-DMA$_{37}$) ($M_{n,SEC}$ = 7600 g·mol^{-1}, $Đ$ = 1.26) recorded in DMSO-d$_6$ at 25 °C.

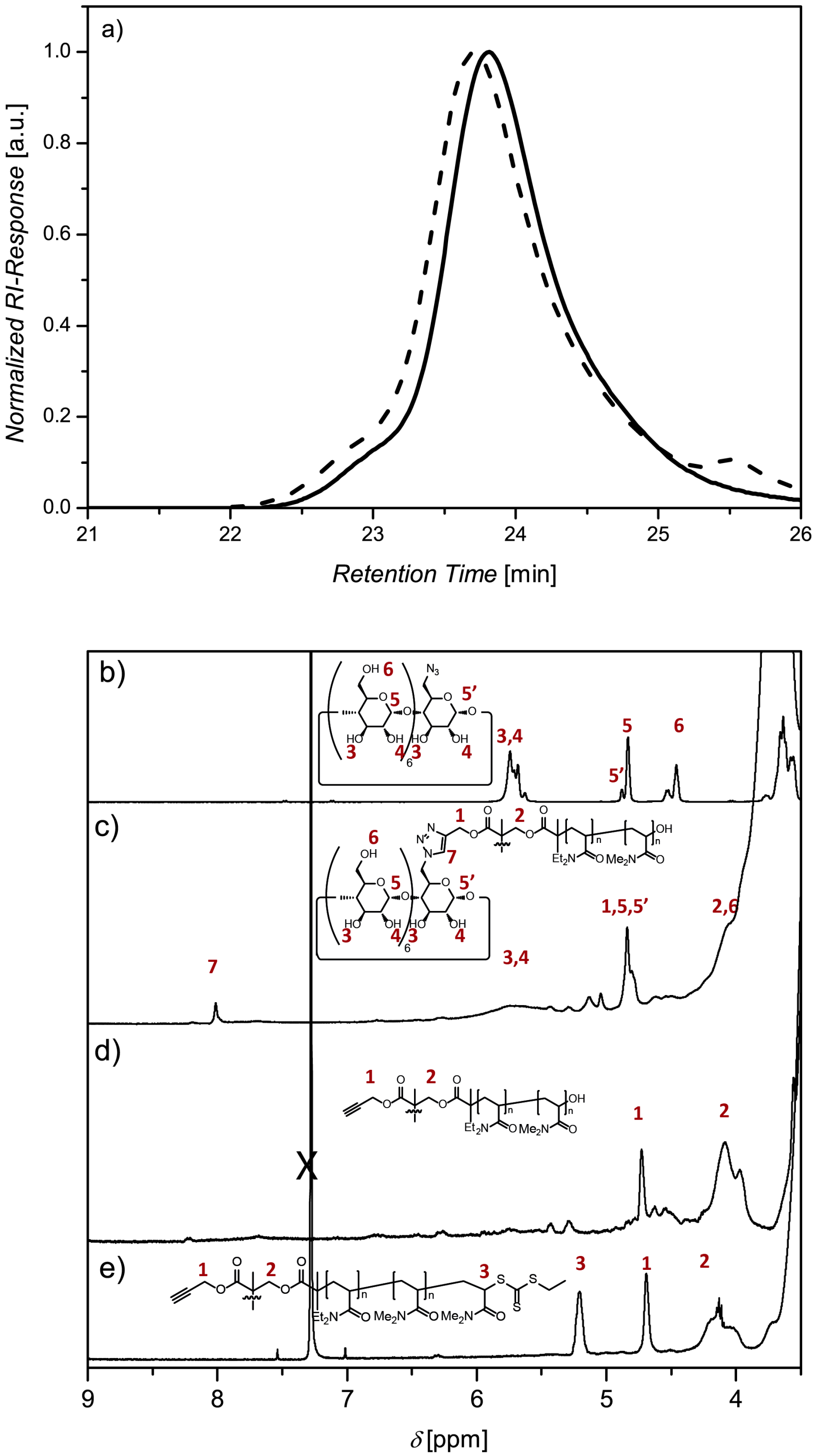

Figure S26. a) SEC Traces of mid-chain alkyne functionalized m-alk-P(DEA$_{39}$-*b*-DMA$_{37}$)-OH (straight line) after RAFT endgroup removal and mid-chain β-CD functionalized m-β-CD-P(DEA$_{39}$-*b*-DMA$_{37}$) (dashed line), magnifications of ^{1}H NMR spectra of b) β-CD-N$_3$, c) m-β-CD-P(DEA$_{39}$-*b*-DMA$_{37}$), d) mid-chain alkyne functionalized m-alk-P(DEA$_{39}$-*b*-DMA$_{37}$)-OH after RAFT endgroup removal and e) mid-chain alkyne functionalized m-alk-P(DEA$_{39}$-*b*-DMA$_{37}$).

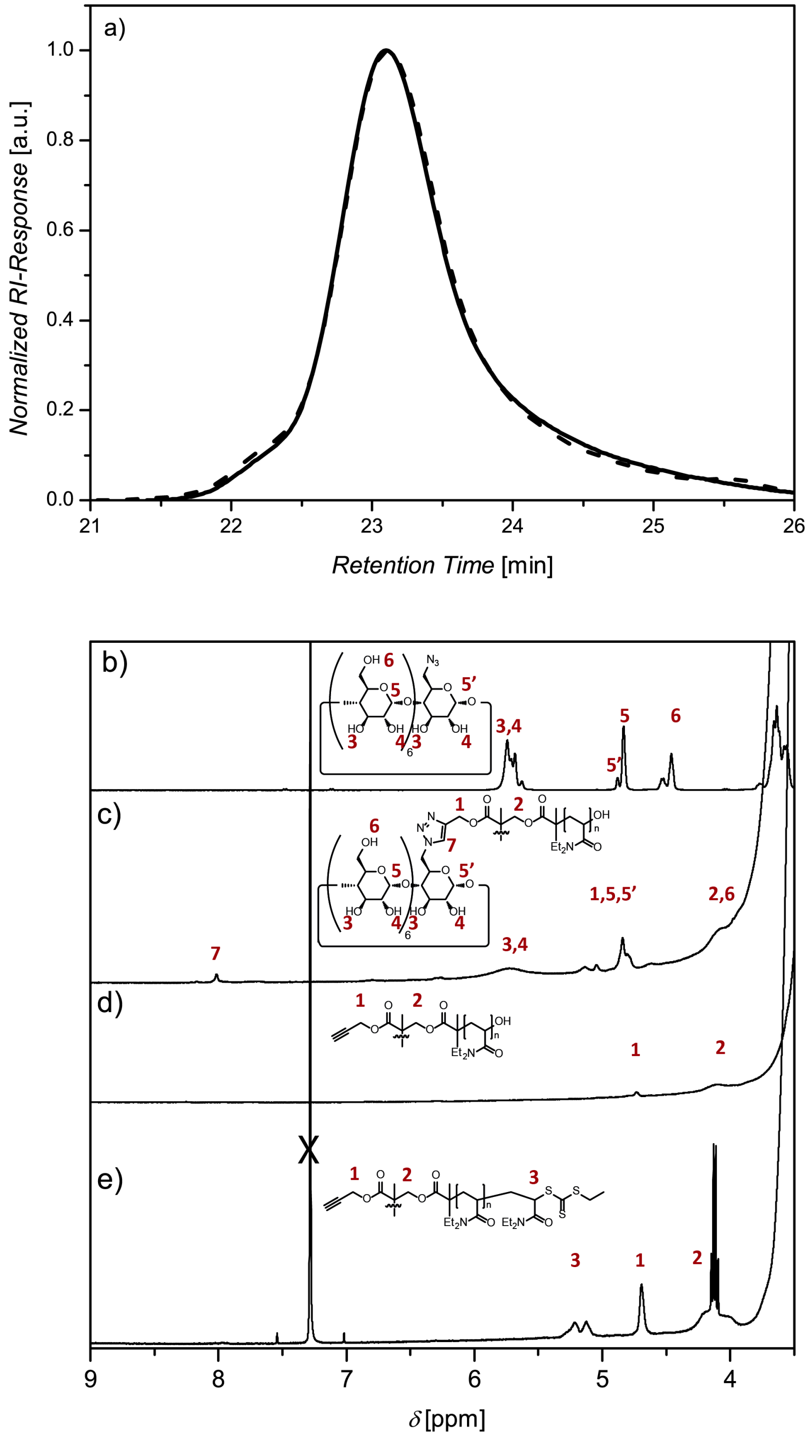

Figure S27. a) SEC Traces of mid-chain alkyne functionalized m-alk-PDEA$_{90}$-OH (straight line) after RAFT endgroup removal and mid-chain β-CD functionalized m-β-CD-PDEA$_{90}$ (dashed line), magnifications of ^{1}H NMR spectra of b) β-CD-N$_3$, c) m-β-CD-PDEA$_{90}$, d) mid-chain alkyne functionalized m-alk-PDEA$_{90}$-OH after RAFT endgroup removal and e) mid-chain alkyne functionalized m-alk-PDEA$_{90}$.

Table S6. Hydrodynamic diameters, D_h, (from the number weighted distributions) of the uncomplexed polymers and the supramolecular complexes in Milli-Q water at a concentration of 1 mg·mL^{-1} at 10 °C.

Sample	D_h [nm]	Std. Dev. [nm]
Ad$_2$-PDMA$_{57}$	18.4	2.5 (12.8%)
Ad$_2$-PDEA$_{51}$	48.7	7.6 (15.5%)
m-Ad-PDMA$_{114}$	6.6	1.0 (15.3%)
m-Ad-PDEA$_{47}$	only slightly soluble	-
m-Ad-P(DEA$_{47}$-*b*-DMA$_{33}$)	19.6	2.6 (13.1%)
m-β-CD-PDMA$_{104}$	2.4	0.2 (9.8%)
m-β-CD-PDEA$_{90}$	75.6	9.8 (12.9%)
m-β-CD-P(DEA$_{39}$-*b*-DMA$_{37}$)	24.7	3.6 (14.7%)
X-Shape		
m-Ad-PDMA$_{114}$-m-β-CD-PDEA$_{90}$	104.5	12.7 (12.1%)
m-β-CD-PDMA$_{104}$-m-Ad-PDEA$_{47}$	10.5	1.5 (14.5%)
m-β-CD-P(DEA$_{39}$-*b*-DMA$_{37}$)-m-Ad-P(DEA$_{47}$-*b*-DMA$_{33}$)	12.5	1.7 (13.4%)
m-β-CD-PDEA$_{90}$-m-Ad-PDEA$_{47}$	21.9	3.0 (13.9%)
m-β-CD-PDMA$_{104}$-m-Ad-PDMA$_{114}$	7.3	0.7 (9.1%)

Sample	D_h [nm]	Std. Dev. [nm]
H-shape		
Ad_2-$PDMA_{57}$-(m-β-CD-$PDEA_{90})_2$	5.3	0.8 (15.3%)
Ad_2-$PDEA_{51}$-(m-β-CD-$PDMA_{104})_2$	4.0	0.4 (11.3%)
Ad_2-$PDEA_{51}$-(m-β-CD-P(DEA_{39}-*b*-$DMA_{37}))_2$	12.2	1.6 (12.8%)
(m-β-CD-$PDEA_{90})_2$-Ad_2-$PDEA_{51}$	9.7	1.2 (12.8%)
(m-β-CD-$PDMA_{104})_2$-Ad_2-$PDMA_{57}$	51.9	6.8 (13.1%)

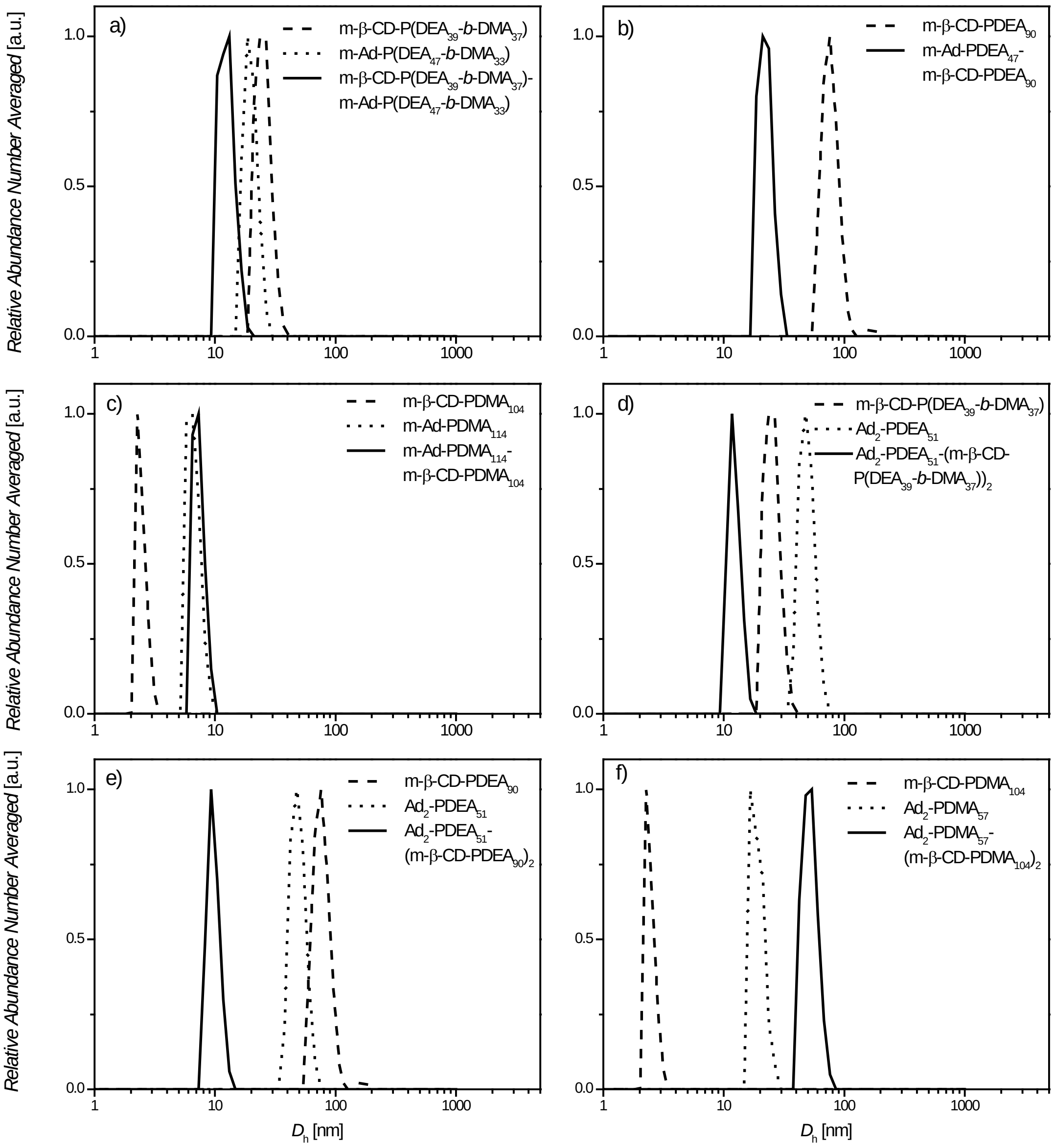

Figure S28. DLS measurements of adamantyl functionalized building blocks (dotted line), CD functionalized building blocks (dashed line) and the supramolecular complex (straight line) at 10 °C and a concentration of 1 mg·mL^{-1} in H_2O: a) X-shape m-β-CD-P(DEA$_{39}$-*b*-DMA$_{37}$), m-Ad-P(DEA$_{47}$-*b*-DMA$_{33}$) and m-β-CD-P(DEA$_{39}$-*b*-DMA$_{37}$)-m-Ad-P(DEA$_{47}$-*b*-DMA$_{33}$), b) X-shape m-β-CD-PDEA$_{90}$ and m-Ad-PDEA$_{47}$-m-β-CD-PDEA$_{90}$ (Note: the block m-Ad-PDEA$_{47}$ is only slightly soluble at 10 °C in H_2O), c) X-shape m-Ad-PDMA$_{114}$, m-β-CD-PDMA$_{104}$ and m-Ad-PDMA$_{114}$-m-β-CD-PDMA$_{104}$, d) H-shape Ad$_2$-PDEA$_{51}$, m-β-CD-P(DEA$_{39}$-*b*-DMA$_{37}$) and Ad$_2$-PDEA$_{51}$-(m-β-CD-P(DEA$_{39}$-*b*-DMA$_{37}$))$_2$, e) H-shape Ad$_2$-PDEA$_{51}$, m-β-CD-PDEA$_{90}$ and Ad$_2$-PDEA$_{51}$-(m-β-CD-PDEA$_{90}$)$_2$ and f) H-shape Ad$_2$-PDMA$_{57}$, m-β-CD-PDMA$_{104}$ and Ad$_2$-PDMA$_{57}$-(m-β-CD-PDMA$_{104}$)$_2$.

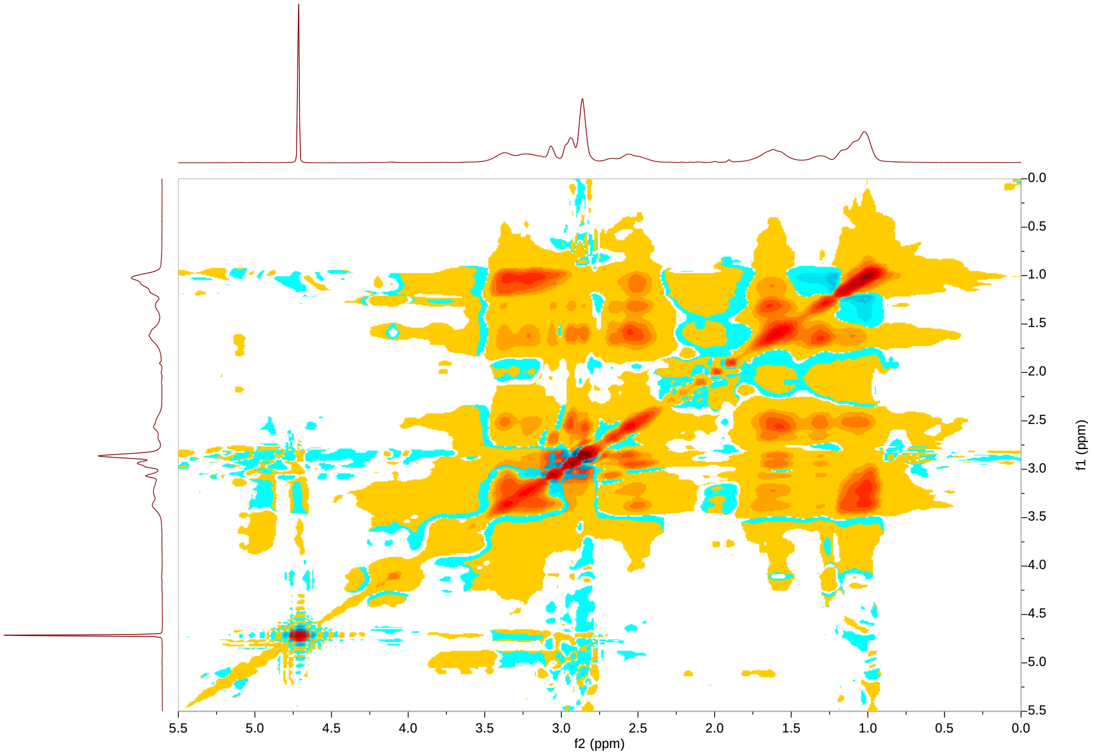

Figure S29. NOESY measurement of X-shape m-β-CD-PDEA$_{90}$-m-Ad-PDMA$_{114}$ in D_2O at 25 °C.

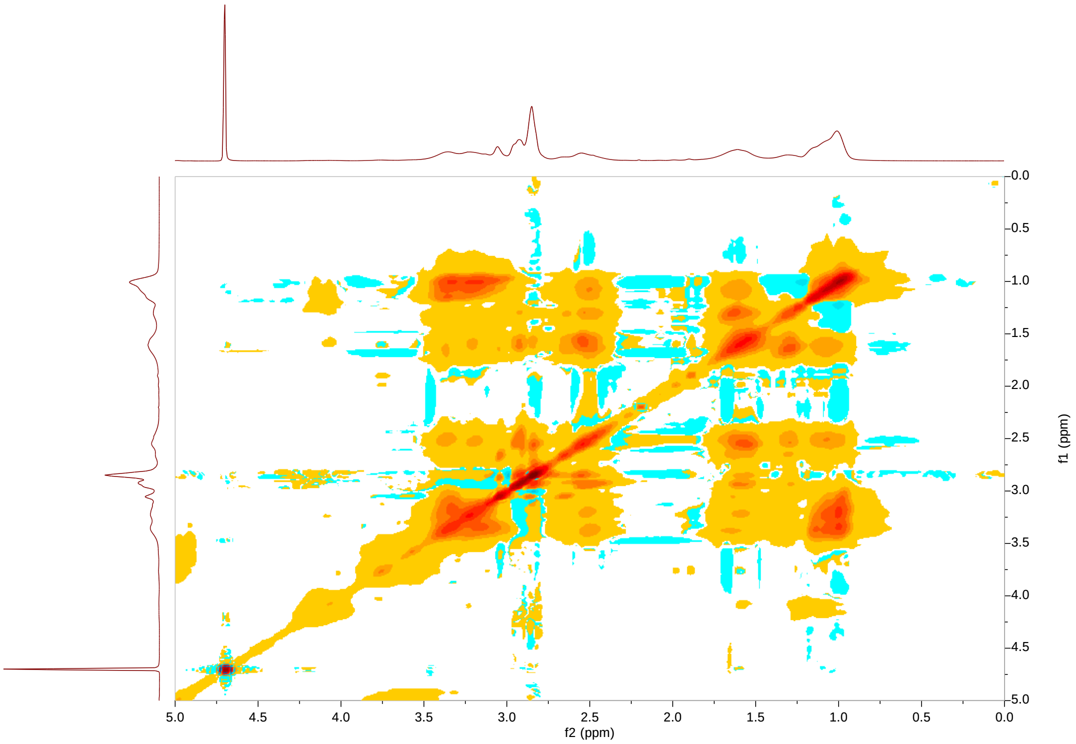

Figure S30. NOESY measurement of X-shape m-β-CD-P(DEA$_{39}$-*b*-DMA$_{37}$)-m-Ad-P(DEA$_{47}$-*b*-DMA$_{33}$) in D_2O at 25 °C.

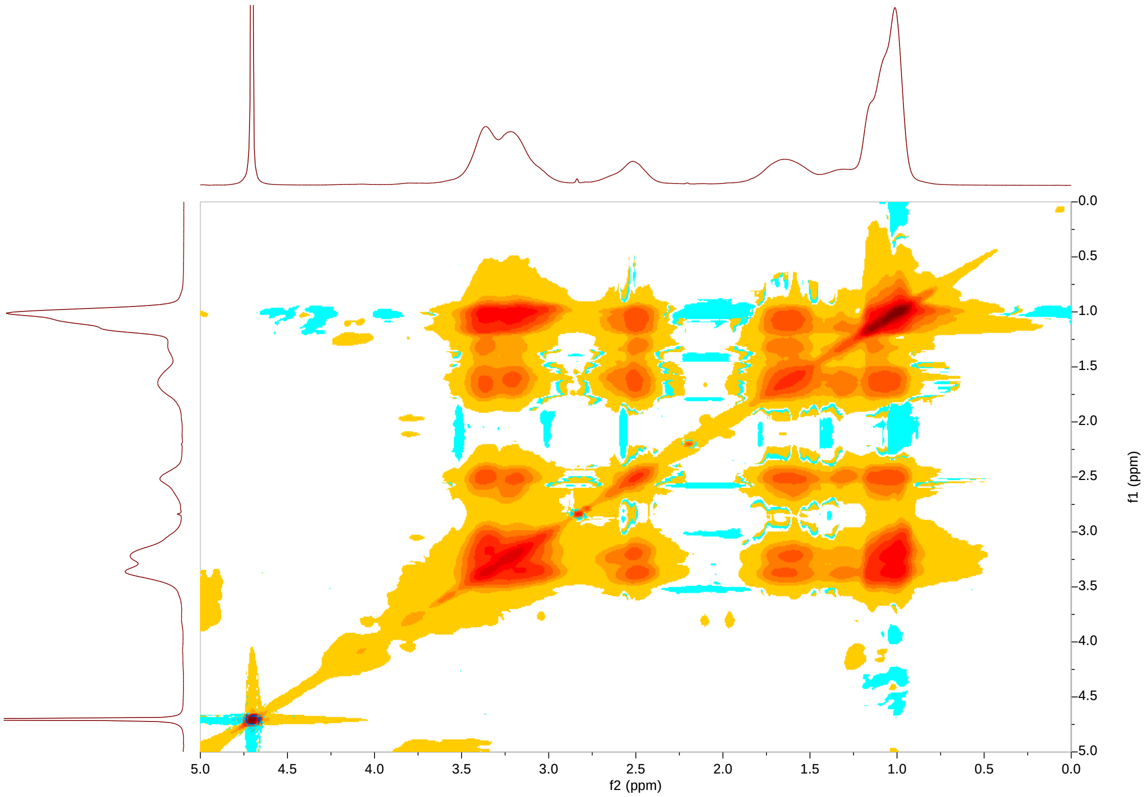

Figure S31. NOESY measurement of X-shape m-β-CD-PDEA$_{90}$-m-Ad-PDEA$_{47}$ in D_2O at 25 °C.

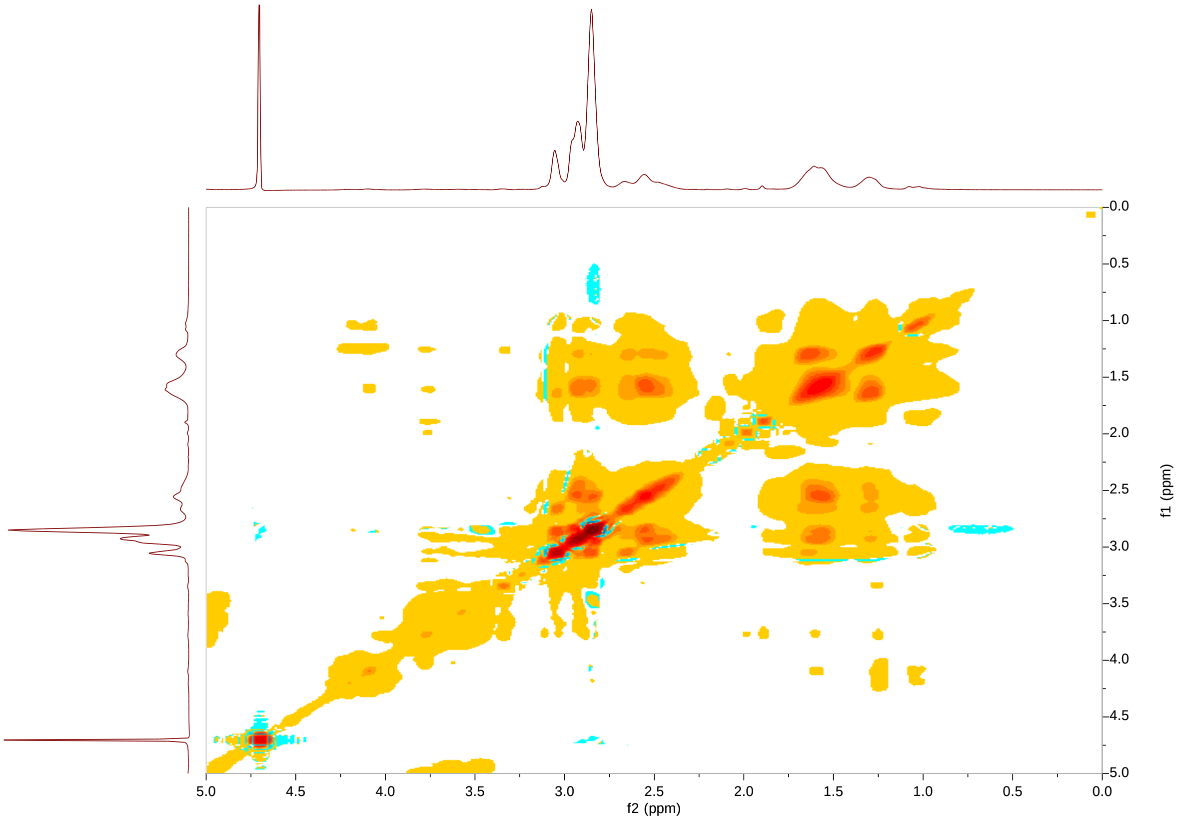

Figure S32. NOESY measurement of X-shape m-β-CD-PDMA$_{104}$-m-Ad-PDMA$_{114}$ in D_2O at 25 °C.

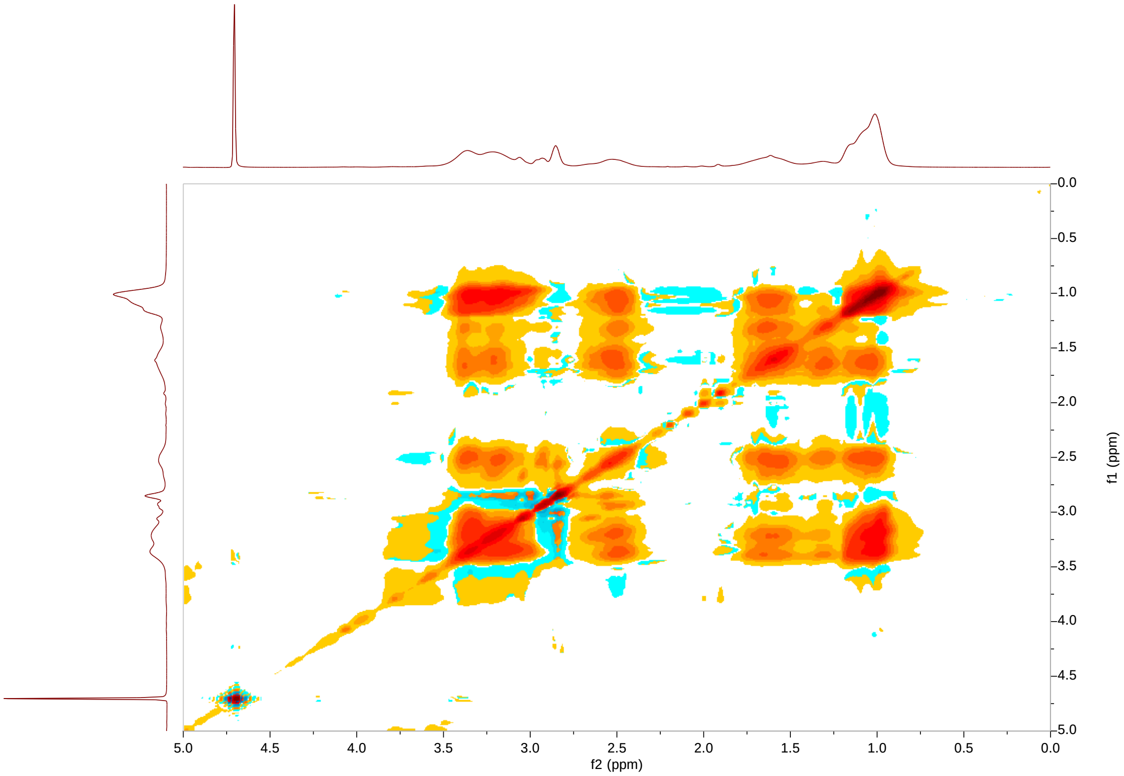

Figure S33. NOESY measurement of H-shape Ad_2-$PDMA_{57}$-(m-β-CD-$PDEA_{90}$)$_2$ in D_2O at 25 °C.

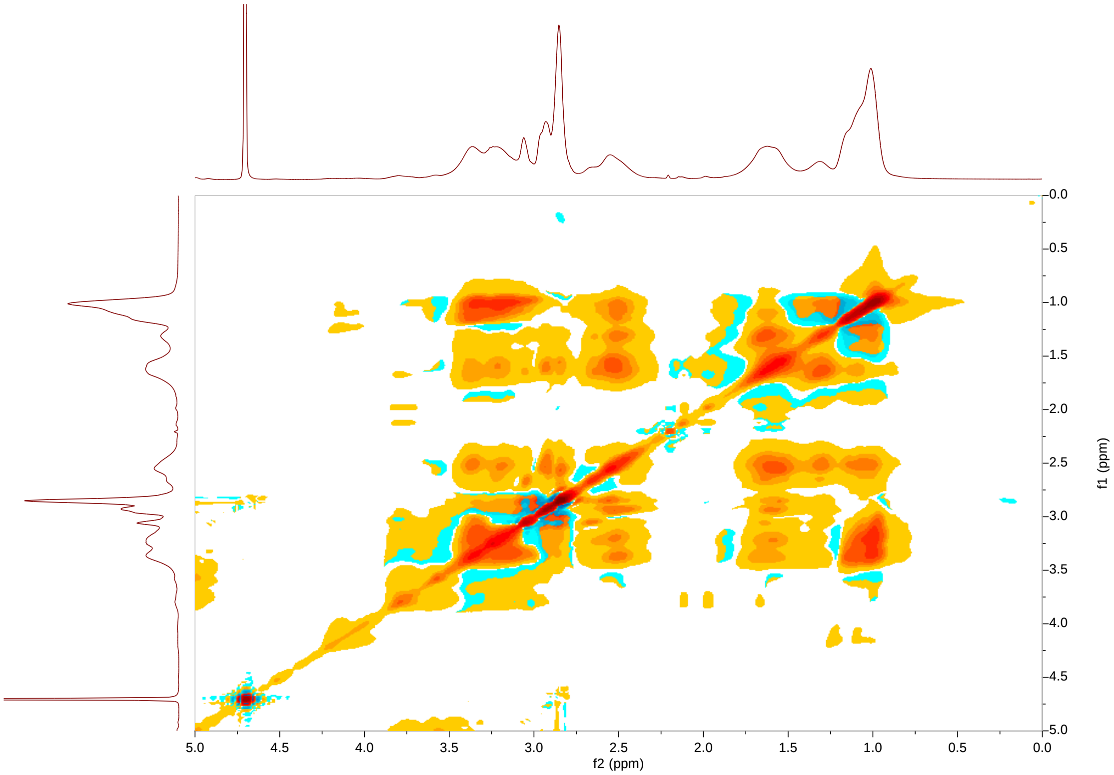

Figure S34. NOESY measurement of H-shape Ad_2-$PDEA_{51}$-(m-β-CD-P(DEA_{39}-*b*-DMA_{37}))$_2$ in D_2O at 25 °C.

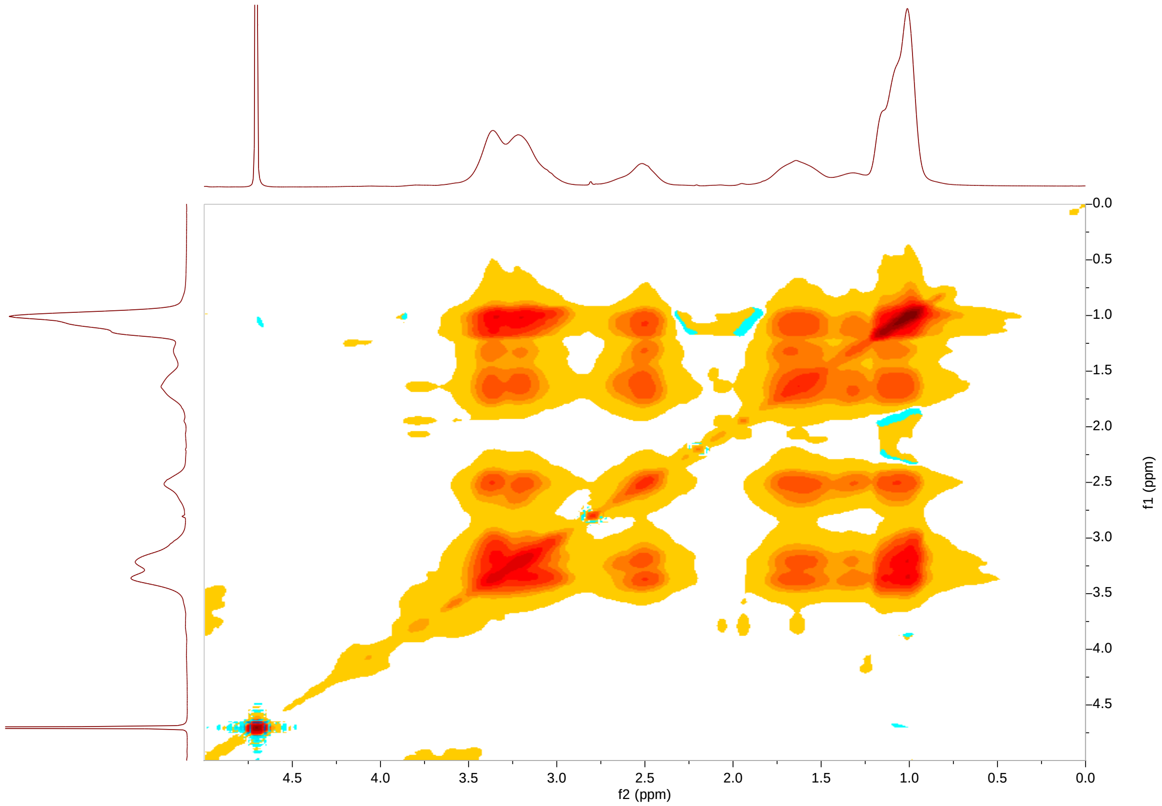

Figure S35. NOESY measurement of H-shape Ad_2-$PDEA_{51}$-(m-β-CD-$PDEA_{90}$)$_2$ in D_2O at 25 °C.

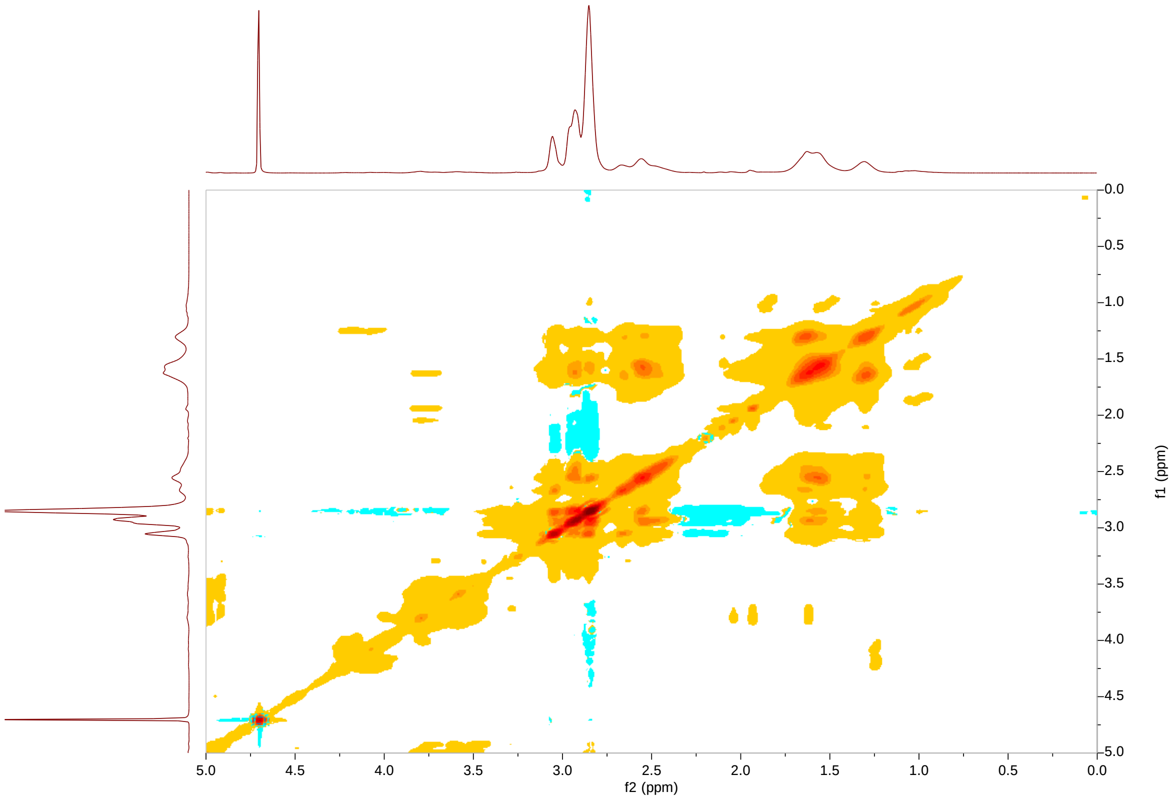

Figure S36. NOESY measurement of H-shape Ad_2-$PDMA_{57}$-(m-β-CD-$PDMA_{104}$)$_2$ in D_2O at 25 °C.

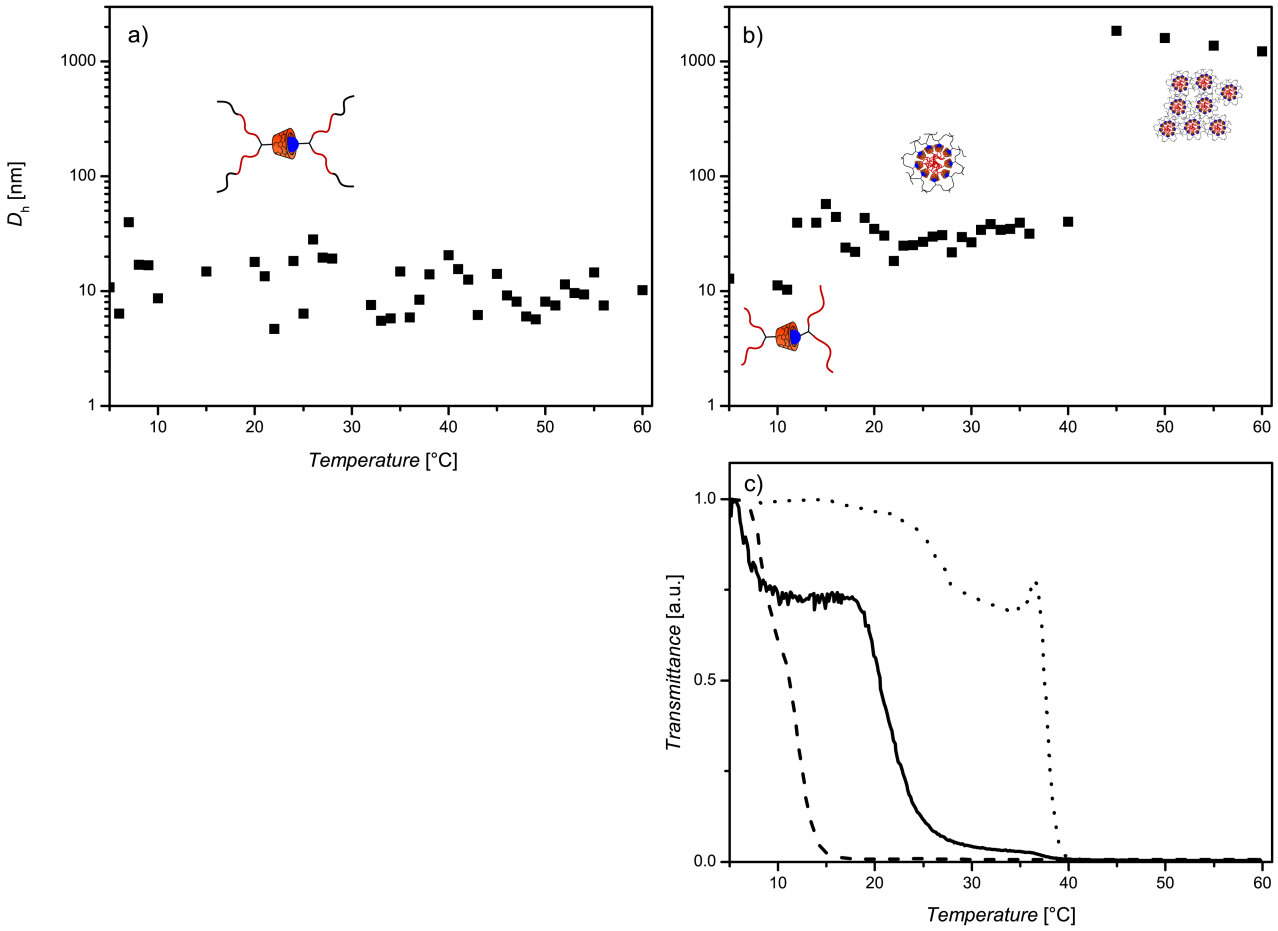

Figure S37. Temperature responsive behavior of X-shape star block copolymers at a concentration of 1 mg·mL^{-1} in H_2O: a) temperature sequenced DLS measurement of m-β-CD-P(DEA$_{39}$-*b*-DMA$_{37}$)-m-Ad-P(DEA$_{47}$-*b*-DMA$_{33}$), b) temperature sequenced DLS measurement of m-β-CD-PDEA$_{90}$-m-Ad-PDEA$_{47}$ and c) turbidimetric measurements of m-β-CD-PDEA (dotted line), m-Ad-PDEA$_{47}$ (dashed line) and m-β-CD-PDEA$_{90}$-m-Ad-PDEA$_{47}$ (straight line).

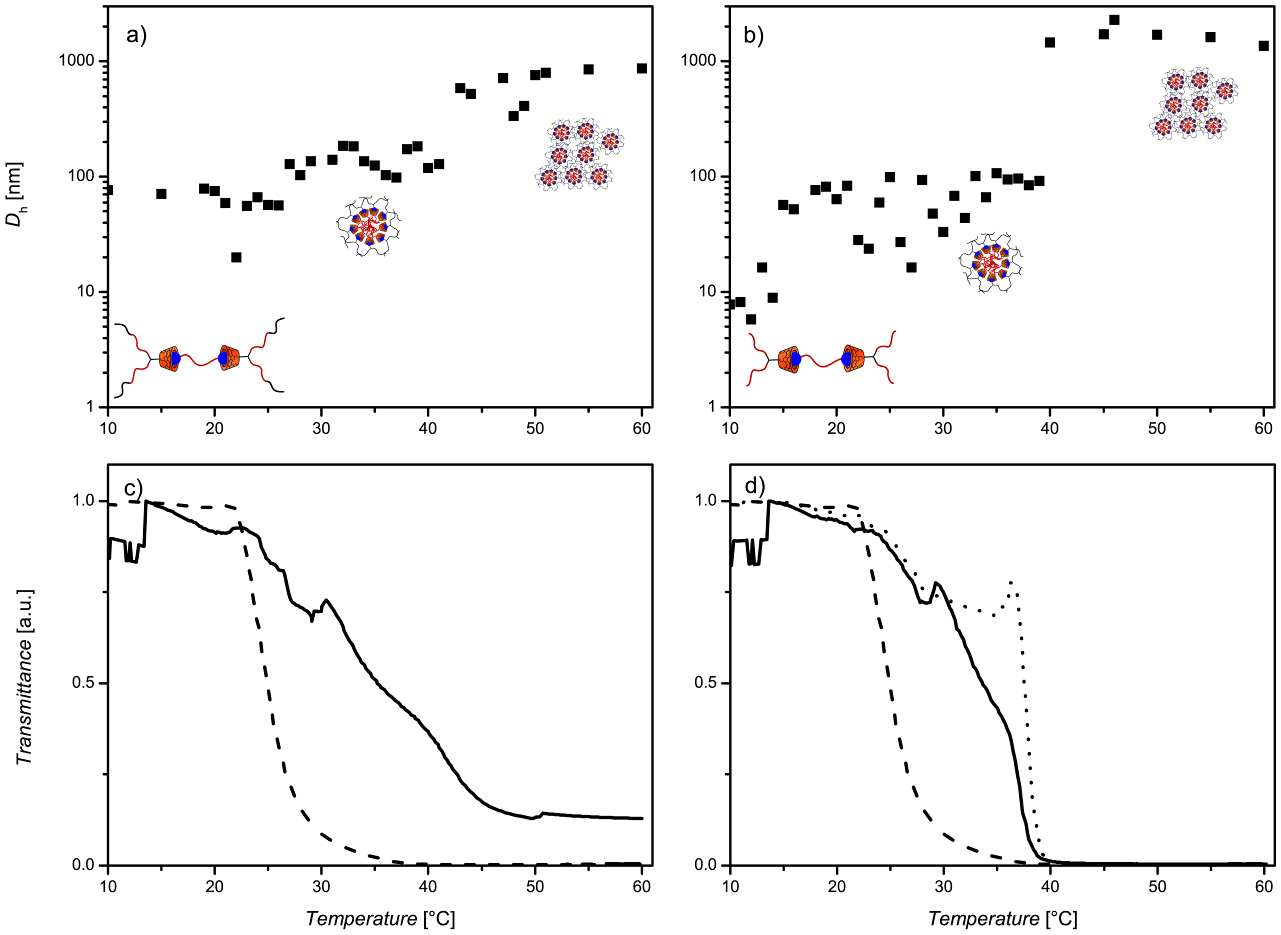

Figure S38. Temperature responsive behavior of H-shape star block copolymers at a concentration of 1 mg·mL^{-1} in H_2O: a) temperature sequenced DLS measurement of Ad$_2$-PDEA$_{51}$-(m-β-CD-P(DEA$_{39}$-*b*-DMA$_{37}$))$_2$, b) temperature sequenced DLS measurement of Ad$_2$-PDEA$_{51}$-(m-β-CD-PDEA$_{90}$)$_2$, c) turbidimetric measurements of Ad$_2$-PDEA$_{51}$ (dashed line) and Ad$_2$-PDEA$_{51}$-(m-β-CD-P(DEA$_{39}$-*b*-DMA$_{37}$))$_2$ (straight line) (Note: m-β-CD-P(DEA$_{39}$-*b*-DMA$_{37}$) shows no cloud point) and d) turbidimetric measurements of m-β-CD-PDEA$_{90}$ (dotted line), Ad$_2$-PDEA$_{51}$ (dashed line) and Ad$_2$-PDEA$_{51}$-(m-β-CD-PDEA$_{90}$)$_2$ (straight line).

Table S7. Cloudpoints (T_cs) of the utilized building blocks and supramolecular star polymers at a concentration of 1 mg·mL^{-1} and a heating rate of 0.32 °C·min^{-1}.

Sample	T_c [°C]
Ad$_2$-PDEA$_{51}$	24.3
m-Ad-PDEA$_{47}$	12.8
m-Ad-P(DEA$_{47}$-*b*-DMA$_{33}$)	no turbidity
m-β-CD-PDEA$_{90}$	37.4
m-β-CD-P(DEA$_{39}$-*b*-DMA$_{37}$)	no turbidity
X-Shape	
m-Ad-PDMA$_{114}$-m-β-CD-PDEA$_{90}$	40.5
m-β-CD-PDMA$_{104}$-m-Ad-PDEA$_{47}$	19.0
m-β-CD-P(DEA$_{39}$-*b*-DMA$_{37}$)-m-Ad-P(DEA$_{47}$-*b*-DMA$_{33}$)	no turbidity
m-β-CD-PDEA$_{90}$-m-Ad-PDEA$_{47}$	20.6
H-shape	
Ad$_2$-PDMA$_{57}$-(m-β-CD-PDEA$_{90}$)$_2$	38.9
Ad$_2$-PDEA$_{51}$-(m-β-CD-PDMA$_{104}$)$_2$	36.0
Ad$_2$-PDEA$_{51}$-(m-β-CD-P(DEA$_{39}$-*b*-DMA$_{37}$))$_2$	slow increase in turbidity
(m-β-CD-PDEA$_{90}$)$_2$-Ad$_2$-PDEA$_{51}$	37.2